Studies on mechanisms of peripheral and central neuropathy in Spontaneously Diabetic Torii (SDT) fatty rats

TATSUYA MAEKAWA

2019

Contents

List of Abbreviations

Abbreviation	Term
AD	Alzheimer's disease
AGE	Advanced glycation endo-product
APP	Amyloid precursor protein
Aβ	Amyloid β
BSB	1-Bromo-2,5-bis(3-carboxy-4- hydroxystyryl)benzene
CA	Cornu ammonis
CNS	Central nervous system
CVD	Cerebroventricular disease
CV_{R-R}	Coefficient of variance of R-R intervals
DM	Diabetes mellitus
DPN	Diabetic peripheral neuropathy
DSM-5	Diagnostic and Statistical Manual of Mental Disorders, Fifth Edition
ECG	Electrocardiogram
ELISA	Enzyme-linked immunosorbent assay
GK	Goto-Kakizaki
HbA1c	Hemoglobin A1c
HE	Hematoxylin and eosin
HSP70-1a	Heat shock 70kD protein 1A
IENFD	Intraepidermal nerve fiber density

Abbreviation	Term
LTP	Long-term potentiation
MNCV	Motor nerve conduction velocity
MRI	Magnetic resonance imaging
NF-κB	Nuclear factor of kappa light polypeptide gene enhancer in B-cells
OLETF	Otsuka Long-Evans Tokushima Fatty
PCR	Polymerase chain reaction
PGP9.5	Protein gene product 9.5
PPARγ	Peroxisome proliferator-activated receptor γ
QOL	Quality of life
S100a9	S100 calcium binding protein A9
SBP	Systolic blood pressure
SD	Sprague-Dawley
SDT	Spontaneously Diabetic Torii
SGLT	Sodium glucose co-transporter
SNCV	Sensory nerve conduction velocity
STZ	Streptozotocin
TC	Total cholesterol
TEM	Transmission electron microscopic
TG	Triglyceride
TNF	Tumor necrosis factor
TSOD	Tsumura Suzuki Obese Diabetes

Abbreviation	Term
VaD	Vascular dementia
ZDF	Zucker Diabetic Fatty

Chapter 1
General Introduction

Peripheral Neuropathy

Diabetic peripheral neuropathy (DPN) is one of the complications induced by diabetes and is manifest as peripheral nerve metabolic disorders and vascular disorders caused by a hyperglycemic state. The incidence of DPN is higher in patients with poor glycemic control, and its prevalence increases with the progression of diabetes mellitus (DM) (Partanen et al., 1995). DPN is classified into sensory motor neuropathy such as numbness, paresthesia, and pain and autonomic disorders such as pupil dysfunction, sweating abnormality, orthostatic hypotension, and gastrointestinal disorders. In regard to the prevalence rate of DPN, Pirart has reported the results of prospective observation of 4400 diabetic patients over 25 years (Pirart, 1978). There were reported that the frequency of complications of neuropathy within 1 year was 7% after diagnosis of DM, the rate is 50% in patients with a disease duration of 25 years or more, and annual incidence rate was 3% to 19% in 25 years. In another large-scale clinical trial, 39% of type 1 DM patients with a disease duration of less than 15 years were reported to have polyneuropathy (The Diabetes Control and Complications Trial Research Group, 1988). The cause of DPN is not singular, and involvement of many factors such as polyol metabolic pathway abnormality, oxidative stress, inflammation, blood flow disorders/vascular endothelial dysfunction, glycation, reduction of neurotrophic factor, and abnormality of protein kinase have been reported (Gabbay et al., 1966; Giugliano et al., 1996; Zhou and Zhou, 2014; Hosseini and Abdollahi, 2013; Callaghan et al., 2012; Tesfaye et al., 2005). The most prevalent cause is polyol pathway abnormality. In the

polyol pathway, a portion of the sugar taken into the nerve cells is metabolized via sorbitol to fructose, and this causes various levels of cytotoxicity (Freeman et al., 2016; Asnaghi et al., 2003). The importance of this pathway is strongly supported, as mice deficient in aldose reductase, which is a converting enzyme from glucose to sorbitol, show only a slight delay in the nerve conduction velocity even when DM develops (Ho et al., 2006). In Japan, the only aldose reductase inhibitor to be used clinically, epalrestat, has been approved, and it suppresses the onset of DPN under good glycemic control (Hotta et al., 2008). However, it is reported that effectiveness is significantly influenced by individual differences, and it is difficult to show effectiveness in patients with high hemoglobin A1c (HbA1c) value or in patients with retinopathy or nephropathy progression (Hotta et al., 2008).

The first choice for the treatment of DPN is glycemic control (Pop-Busui et al., 2017). There is no global therapeutic agent available, but symptomatic treatment for positive symptoms such as pain and numbness accompanying onset of neurological disorder is selected next to glycemic control. However, all of these are symptomatic treatments, not therapeutic agents based on the cause, and an effective therapeutic approach for the treatment of DPN is lacking.

DPN has been reported in some diabetic animal models (Islam, 2013). For example, diabetic model mice and rats established by disrupting pancreatic β cells by administration of streptozotocin (STZ), genetically diabetic C57BL/Ks (*db/db*) mice, and WBN/Kob rats are being used (Filho and Fazan, 2006; Vareniuk et al., 2008; Murakami et al., 2013; Hinder et al., 2013; Yagihashi et al., 1993). Decrease in the sensory nerve conduction velocity (SNCV) and motor nerve conduction velocity (MNCV), histopathological changes such as the loss of intraepidermal nerve fiber or

structural demyelination were observed. However, autonomic nerve function has not been analyzed in these model animals, and adequate validation has not been carried out using antineuropathic drugs or antidiabetic drugs. Also, the onset of DPN in these animals is observed in a relatively old age. Pathophysiological analysis in diabetic animal models is important for the development of novel therapies for DPN. In Chapter 2, the mechanism of DPN was investigated using the obese type 2 diabetic model to elucidate a new strategy for DPN treatment.

Central Neuropathy

From a perspective of the central nervous system (CNS), reports on the relationship between DM and neurodegenerative diseases such as dementia are increasing annually. It is reported that DM is an acquired risk factor for Alzheimer's disease (AD) in some residential cohort studies (Ott et al., 1999; Leibson et al., 1997; Peila et al., 2002; Yoshitake et al., 1995; Ohara et al., 2011). Also, in some meta-analyzes, cognitive impairment in children and adults with type 1 DM has been reported (Gaudieri et al., 2008; Brands et al., 2005).

Dementia includes a variety of causative diseases and conditions. According to the Diagnostic and Statistical Manual of Mental Disorders, Fifth Edition, published by the American Psychiatric Association (DSM-5, Arlington, VA: APA; 2013), the pathogenesis of dementia is classified into AD, Lewy body disease, vascular disease, frontotemporal lobar degeneration, traumatic brain injury, Parkinson’s disease, Huntington’s disease, and others (Patterson, 2018). Among these, vascular dementia (VaD) and Alzheimer’s dementia account for the majority of all dementia patients. VaD is dementia caused by cerebroventricular disease (CVD), accounting for about 20 to

30% of the total cases of dementia (Patterson, 2018). On the other hand, Alzheimer's dementia accounts for 50 to 60% of all cases (Patterson, 2018). Alzheimer's dementia is characterized by two changes of pathological neurofibrillary tangles and amyloid β (Aβ) accumulation (Duyckaerts et al., 2009). Neuronal cell death, synapse reduction, and decline of choline acetyltransferase activity, which is acetylcholine synthase, then occur in the cerebral cortex, hippocampus, and other areas, resulting in dementia (West et al., 1994; DeKosky and Scheff, 1990; Davies and Maloney, 1976; Bowen et al., 1976).

Although the cause of AD onset has not been completely elucidated, it is thought that multiple intertwined factors such as aging, genetic factors, and lifestyle habitual factors are responsible (Biessels et al., 2006). Lifestyle-related diseases, especially DM, are risk factors for dementia as described above. In addition to cerebrovascular lesions such as arteriosclerosis and microvascular disease accompanying DM, metabolic lesions such as oxidative stress, advanced glycation end-products (AGEs) caused by glucose toxicity, and impaired insulin signaling in insulin metabolism have been estimated as factors that increase the risk of developing dementia by diabetes (Biessels et al., 2006).

As animal models related to dementia, a model with artificially induced brain damage, a senescence accelerated model, and a genetic modification model are used (Miyamoto et al., 1985; Takeda et al., 1981; Hsiao et al., 1996). As AD models related to glucose metabolism abnormality, STZ- or high fat diet-treated transgenic or normal animals and a spontaneously diabetic model are used (Jolivalt et al., 2010; Ho et al., 2004; Li et al., 2007). For example, accumulation of phosphorylated tau and Aβ in the brain was observed in amyloid precursor protein (APP) transgenic mice treated with STZ (Jolivalt et al., 2010). It was reported that the high fat diet regulated insulin

degrading enzyme activity and γ-secretase activity to promote Aβ pathology in Tg2576 mice (Ho et al., 2004). In prediabetic type 2 BBZDR/Wor rats and in type 1 BB/Wor rats, it is reported that the expression of phosphorylated tau and Aβ occurred in association with insulin resistance and hypercholesterolemia (Li et al., 2007). So far, novel therapies and therapeutic drugs for central neuropathy using these model animals have not been developed, and thus it is very important for the development of new therapies to elucidate the pathology of central neuropathy in a novel DM model. Therefore, in Chapter 3, mechanism of central neuropathy was investigated using the obese type 2 diabetic model to elucidate a new strategy for central neuropathy treatment.

Spontaneously Diabetic Torii fatty rat

The Spontaneously Diabetic Torii (SDT) fatty rat is a congenic strain of an SDT rat with the *fa* allele of the leptin receptor gene (*Lepr*^{fa}). This rat was established by insertion of the *Lepr*^{fa} gene of the Zucker fatty rat into the genome of the SDT rat, an inbred model of non-obese type 2 DM, through the speed congenic method (Masuyama et al., 2005). The SDT fatty rat is a model for obese type 2 DM showing overt obesity, hyperglycemia, and hyperlipidemia from a young age, and the three major complications of DM in kidneys, eyes, and nerves (Matsui et al., 2008; Yamaguchi et al., 2012; Katsuda et al., 2015). Furthermore, SDT fatty rats showed the decreased tail MNCV and decrease in the number of sural nerves at 40 weeks of age (Yamaguchi et al., 2012). However, studies on the pathogenesis and mechanism of the development and progression of DPN, including early onset and drug responsiveness, in SDT fatty rats have not been performed in detail. On the other hand, various reports on DM and

dementia suggest that neuropathy in CNS may also occur in SDT fatty rats; however, there is no research on the central neuropathy of SDT fatty rats. Unlike other animal models, SDT fatty rats develop diabetic retinopathy such as the retinal dysfunction and histopathological abnormalities, including retinal folding, retinal thickening, and mature cataracts, and findings of diabetic nephropathy such as glomerulosclerosis and tubular pathology (Katsuda et al., 2015; Motohashi et al., 2018). Pathophysiological analysis using SDT fatty rats may be able to provide useful information against DPN and CNS disorders that lack an effective treatment method or for which there is insufficient clarification of pathology.

Purpose

In the present study, analyses of physiological functions and histopathological changes were performed to elucidate the pathophysiological features of the development and progression of DPN in the SDT fatty rat. Furthermore, physiological and histopathological analyses of brain were performed to clarify the features of the central neuropathy in aged SDT fatty rats.

Chapter 2

Pathophysiological profiles of SDT fatty rats, a potential new diabetic peripheral neuropathy model

INTRODUCTION

The three major complications of DM include diabetic retinopathy, diabetic nephropathy, and DPN, and approximately 50% of DM patients have serious complications (Galuppo et al., 2014). Glycemic control is the first choice for the treatment of DPN. In clinical practice, strict control of blood glucose suppressed delayed nerve conduction velocity and deteriorations of the vibratory perception threshold in type 2 DM patients (Ohkubo et al., 1995). In addition, even in the Diabetes Control and Complication Trial (DCCT) targeting type 1 DM patients, the onset of neuropathy was significantly suppressed with the control of blood glucose (The Diabetes Control and Complications Trial Research Group, 1993, 1995). On the other hand, epalrestat, which is approved in Japan as an aldose reductase inhibitor, is the only treatment based on the cause of DPN. Epalrestat reportedly suppresses the development of DPN under conditions of good glycemic control (Hotta et al., 2008). However, inhibiting a single metabolic parameter is not sufficient to treat DPN (Yagihashi et al., 2011), and it seems that unmet medical needs are still high for therapeutic agents for DPN. In the pharmaceutical industry, appropriate animal models are essential for the development of new drug candidates for DPN and, in particular, animal models showing DPN at an early stage are needed.

SDT fatty rats are a useful animal model for investigating diabetic complications because SDT fatty rats show the three major complications of DM in

kidneys, eyes, and nerves (Matsui et al., 2008; Ishii et al., 2010a; Katsuda et al., 2015; Yamaguchi et al., 2012). The onset of DPN is observed in over 50% of all patients with type 1 and type 2 DM (Pop-Busui et al., 2009) and various animal models for DPN have been reported (Islam, 2013), whereas there are few reports using SDT fatty rats for DPN. It was reported that MNCV was delayed in SDT fatty rat at 24 weeks of age, and the number of sural nerve fibers tended to be reduced in SDT fatty rats at 24 weeks of age, but a significant reduction was observed at 40 weeks of age (Yamaguchi et al., 2012). There have been a few reports of sufficient histopathological analyses performed on the peripheral nerves of obese rats. These analyses are necessary to advance the histological analysis of type 2 DM rats (Katsuda et al., 2014). Therefore, in the present study, we investigated the development of DPN at an early stage in SDT fatty rats using functional analyses, such as nerve conduction velocity, blood pressure, electrocardiogram (ECG) and pupil size, and morphological analyses such as intraepidermal nerve fiber density (IENFD) and transmission electron microscopic (TEM) analysis. Abnormalities in the peripheral nerves, both sensory/motor nerves and autonomic nerves, of SDT fatty rats were investigated thoroughly to elucidate the utility of these animals as a model for peripheral neuropathy.

MATERIALS AND METHODS

Animals

Male SDT$^{fa/fa}$ (SDT-*Lepr*^{fa} or SDT fatty) rats (Clea Japan, Tokyo, Japan) were used in the study. At 4 weeks of age, SDT fatty rats were divided into two groups (n=6), a phlorizin or a vehicle-treated (control) group. Age-matched male Sprague-Dawley (SD) rats (Clea Japan, Tokyo, Japan) were used as normal animals (n=6). Animals were

housed in a climate-controlled room (temperature 23 ± 3°C, humidity 55 ± 15%, 12h lighting cycle) and allowed free access to basal diet (CRF-1 powder, Oriental Yeast, Tokyo, Japan) and sterilized water. All animal protocols used in the study were in strict compliance with our own Laboratory Guidelines for Animal Experimentation and were approved by the Institutional Animal Care and Use Committee of Central Pharmaceutical Research Institute, Japan Tobacco Inc. All functional tests (except for blood pressure measurement) were performed under sodium pentobarbital/diazepam or isoflurane anesthesia, and all efforts were made to minimize suffering.

Treatments

Phlorizin (Kanto chemical, Tokyo, Japan), a sodium-glucose co-transporter (SGLT) inhibitor, was used as a glycemic control agent, and the drug was suspended in 20% propylene glycol. The vehicle (20% propylene glycol) or phlorizin were injected subcutaneously once daily to rats for 12-weeks period, from 5 to 16 weeks of age. The dose of phlorizin was started at 100 mg/kg and switched to 150 mg/kg from 8 weeks of age, because the plasma glucose level in phlorizin-treated group was not well-controlled at 6 weeks of age.

Measurement of biochemical parameters

Body weights were measured one or more times a week. Biochemical parameters such as plasma glucose, insulin, triglyceride (TG), and total cholesterol (TC) levels, and HbA1c were measured at 4, 5, 8, 10, 12 and 16 weeks of age in the non-fasting state. Blood samples were collected from the subclavian vein of the rats at 4 to 12 weeks of age. At the end of the treatment period (16 weeks of age), blood samples

were collected from the abdominal aorta of rats under isoflurane anesthesia. Plasma glucose, TG, TC and HbA1c were measured using commercial kits (Roche Diagnostics, Basel, Switzerland) and an automatic analyzer (HITACHI Clinical analyzer 7180; Hitachi, Tokyo, Japan). Plasma insulin levels were measured using rat insulin enzyme-linked immunosorbent assay (ELISA) kits (Morinaga Institute of Biological Science, Yokohama, Japan).

Measurement of sciatic nerve conduction velocity

Sciatic nerve conduction velocity was measured at 15 weeks of age (Figure 1). Rats were anesthetized with an intraperitoneal injection of sodium pentobarbital (37.5 mg/kg, Kanto chemical, Tokyo, Japan) and diazepam (3 mg/kg, Maruishi Pharmaceutical Co., Osaka, Japan). The left sciatic nerve was electronically stimulated with 0.2 ms pulses (supramaximal voltage: approximately 3.5 V) via fine percutaneous needle electrodes placed at the sciatic notch and the Achilles tendon. The action potentials derived from motor nerve stimulation (M-waves) or sensory nerve stimulation (F-wave) were recorded via PowerLab (ADInstruments, USA) through fine needle electrodes placed on dorsalis pedis. The peak latencies of F-waves and M-wave were measured and automatically calculated as the intervals between the onset of the stimulus and the peaks of both F-wave and M-waves in the Achilles tendon and the sciatic notch using a software (Scope, ADInstruments). The nerve length between the electrodes which were placed on the Achilles tendon and sciatic notch was measured by a vernier caliper. The formulas used to calculate SNCV and MNCV were as follows.

SNCV (m/sec) = distance between the sciatic nerve and Achilles tendon (mm) / (peak latency of an F-wave in the Achilles tendon – peak latency of an F-wave in the

sciatic notch) (msec)

MNCV (m/sec) = distance between the sciatic nerve and Achilles tendon (mm) / (peak latency of an M-wave in the sciatic notch – peak latency of an M-wave in the Achilles tendon) (msec)

Measurement of electrocardiograms, blood pressure, and pupil size

As an autonomic nerve function test, the coefficient of variance of R-R intervals ($CV_{R\text{-}R}$) obtained from ECG, blood pressure, and pupil size were measured at 15 weeks of age. ECG were recorded using a data acquisition system (PowerLab 8/30 system, ADInstruments, USA) and LabChart software (Version 7, AD Instruments, USA) under mild isoflurane anesthesia. To calculate $CV_{R\text{-}R}$, the standard deviation for the R-R interval for a heart rate of 300 immediately prior to the cessation of anesthesia was divided by the average of R-R intervals. Systolic blood pressure (SBP) in the conscious state was measured using the indirect tail cuff method using Softron BP-98A (Softron, Tokyo, Japan). The pupil size of both eyes was measured using a stereo microscope under mild isoflurane anesthesia before and 30 minutes after the instillation of mydriatic drops (mydrin P, Santen Pharmaceutical Co., Ltd., Japan).

Histology

At the end of the treatment period (16 weeks of age), all animals were perfused with 4% paraformaldehyde after the blood sample collection under isoflurane anesthesia. Sural nerves were fixed in 4% glutaraldehyde/10% neutral-buffered formalin. The processing for TEM was as follows: isolated sural nerves were immersed in an ice-cold mixture of 0.1 mol/L phosphate buffered 2% paraformaldehyde and 1.25%

glutaraldehyde overnight. The fixed tissues were trimmed to cross-sections and were fixed in 0.1 mol/L phosphate buffered 2% osmium tetroxide. After being dehydrated in serial ethanol solutions at graded concentrations, the tissues were embedded in epoxy resin (Quetol-651, Nissin EM, Tokyo). Thin sections of representative areas selected for electron microscopy were stained with uranyl acetate and lead citrate, and were then observed under a transmission electron microscope (model HT7700, Hitachi, Tokyo).

Immunohistochemistry

To evaluate small fiber neuropathy, IENFD was measured in accordance with a previous report (Katsuda et al., 2015). The plantar skin of the left hind limbs of animals was dissected and fixed in 4% PFA, embedded in paraffin, and sectioned (25 μm). Nerve fibers were immunostained for protein gene product 9.5 (PGP 9.5; rabbit polyclonal, 1:500; UltraClone, Isle of Wight, U.K.) overnight at 4°C and subsequently with Alexa Fluor® mouse anti-rabbit IgG antibody 488 (1: 1,000, Thermo Fisher Scientific, Waltham, MA, USA) for 30 min at room temperature. Five fields from each section were randomly selected and Z-stack images were obtained using a Nikon A1 confocal laser scanning microscope mounted on an inverted microscope (Eclipse Ti, Nikon, Tokyo, Japan). Nerve fibers with branching inside the epidermis were considered one nerve. IENFDs were expressed as numbers of epidermal nerve fibers per length of the epidermal basement membrane (fibers/mm). The measurement of IENFD was performed by one controlling person and one blinded observer.

Statistical analysis

Results are expressed as means ± standard deviations. For statistical

evaluations, a one-way ANOVA followed by a Student's *t*-test or Aspin-Welch's *t*-test were performed at each time point. In all cases, $p < 0.05$ was considered statistically significant.

RESULTS

Body Weight and Biochemical Parameters

The body weights of vehicle-treated (control) SDT fatty rats were significantly higher than that of age-matched SD rats during the treatment period. Phlorizin-treated SDT fatty rats were heavier than vehicle-treated (control) SDT fatty rats after 14 weeks of age (after 9 weeks of treatment) (body weight at 16 weeks of age: SD group, 504 ± 60 g; control group, 590 ± 40 g; phlorizin group, 688 ± 46 g, respectively) (Figure 2A). The plasma TG and TC levels of vehicle-treated (control) SDT fatty rats were higher than that of SD rats. Plasma TG and TC levels in the phlorizin-treated group were significantly lower than that of the vehicle-treated (control) group during the treatment period (TG levels at 16 weeks of age: SD group, 130 ± 33 mg/dL; contrl group, 498 ± 115 mg/dL; phlorizin group, 275 ± 55 mg/dL, respectively, TC levels at 16 weeks of age: SD group, 63 ± 14 mg/dL; control group, 116 ± 25 mg/dL; phlorizin group, 89 ± 7 mg/dL, respectively) (Figures 1B and 1C). The plasma glucose levels of vehicle-treated (control) SDT fatty rats were higher than that of SD rats at 4 weeks of age (before treatment). These gradually increased to approximately 600 mg/dL at the end of treatment period (Figure 2D). Although the plasma glucose levels of the phlorizin-treated SDT fatty rats temporarily increased at 6 weeks of age, the appropriate dose increase from 100 mg/kg to 150 mg/kg of phlorizin at 8 weeks of age controlled plasma glucose levels from then on, and the glucose levels decreased to levels that were

equivalent to that of SD rats at the end of treatment period (glucose levels at 16 weeks of age: SD group, 238 ± 26 mg/dL; control group, 618 ± 53 mg/dL; phlorizin group, 238 ± 78 mg/dL, respectively) (Figure 2D). The fluctuations in HbA1c levels reflected the change in blood glucose level accurately (Figure 2E). The plasma insulin levels of vehicle-treated (control) SDT fatty rats were significantly higher than that of SD rats at the beginning of treatment (5 weeks of age) and gradually decreased to normal levels at 16 weeks of age. Phlorizin treatment delayed insulin decreases and insulin remained high even at the end of treatment (insulin levels at 16 weeks of age: SD group, 1.7 ± 1.7 ng/mL; control group, 3.7 ± 0.9 ng/mL; phlorizin group, 14.7 ± 11 ng/dL, respectively) (Figure 2F).

Sciatic nerve conduction velocity

SNCV was significantly delayed, while MNCV was partly delayed in vehicle-treated (control) SDT fatty rats (SNCV; 39.9 ± 5.4 m/s, MNCV; 41.2 ± 8.5 m/s) compared with age-matched SD rats (SNCV; 59.1 ± 4.0 m/s, MNCV; 49.3 ± 12.7 m/s) at 15 weeks of age. The SNCV of SDT fatty rats decreased to 67.5% of that in SD rats and MNCV decreased to 83.5% (Figure 3). These functional impairments in sciatic nerves improved with phlorizin treatment (SNCV; 56.1 ± 9.2 m/s, MNCV; 57.9 ± 8.0 m/s).

IENFD and morphological abnormalities

IENFD from the skin of the hind paw foot of vehicle-treated (control) SDT fatty rats slightly decreased at 16 weeks of age (SD rats, 29.7 ± 9.6 fibers/mm; SDT fatty rats, 22.8 ± 4.9 fibers/mm). Phlorizin treatment tended to prevent decreases in nerve fibers (26.8 ± 4.1 fibers/mm) (Figure 4). In TEM analyses, the mitochondrial abnormalities

(swelling or degeneration) of small myelinated fibers (3 out of 6 rats), and the vacuolation (4 out of 6 rats) and mitochondrial swelling (4 out of 6 rats) of unmyelinated fibers were found in vehicle-treated (control) SDT fatty rats but not age-matched SD rats (Table 1 and Figure 5). Phlorizin treatment clearly resolved these morphological abnormalities. The mitochondrial abnormalities of small myelinated fibers, vacuolation and mitochondrial swelling of unmyelinated fibers were founded in 0, 1 and 2 out of 6 rats in phlorizin-treated group, respectively. The number of those findings decreased with phlorizin treatment. However, the thinning of the myelin sheaths of small myelinated fibers were founded in all of vehicle (control)- and phlorizin-treated SDT fatty rats.

Autonomic nerve function

The $CV_{R\text{-}R}$ partly decreased, while SBP was significantly elevated in vehicle-treated (control) SDT fatty rats ($CV_{R\text{-}R}$; 1.26 ± 0.27%, SBP; 142.2 ± 15.2 mmHg) compared with age-matched SD rats ($CV_{R\text{-}R}$; 2.56 ± 1.46%, SBP; 114.2 ± 8.9 mmHg) at 15 weeks of age (Figures 6A and 6B). These changes improved with phlorizin treatment ($CV_{R\text{-}R}$; 2.08 ± 0.76%, SBP; 117.0 ± 4.2 mmHg). Before and after the instillation of mydriatic drops, the pupil size of both eyes of SDT fatty rats were smaller than that of age-matched SD rats (Figure 6C). Before the instillation, the pupil size of the right and left eyes in the vehicle-treated (control) SDT fatty rats were 0.48 ± 0.17 and 0.45 ± 0.20 mm, respectively, and those in the age-matched SD rats were 0.72 ± 0.15 and 0.69 ± 0.19 mm, respectively. After the instillation, the pupil size of the right and left eyes in the vehicle-treated (control) SDT fatty rats were 4.84 ± 0.31 and 4.72 ± 0.26 mm, respectively, and those in the age-matched SD rats were 5.31 ± 0.23 and 5.28 ± 0.17

mm, respectively. Phlorizin improved pupil size after the instillation of mydriatic drops (right and left: 5.06 ± 0.41 and 5.04 ± 0.42 mm, respectively). However, there were no changes before the instillation.

DISCUSSION

In the previous study, male SDT fatty rats showed signs of diabetic neuropathy, such as a decrease in tail MNCV and the number of sural nerve fibers, after 24 weeks of age (Yamaguchi et al., 2012). In the present study, to clarify the relationship between functional and morphological changes to the peripheral nerves, measurements of nerve conduction velocity and IENFD, and TEM analyses of peripheral nerves were performed using young (before 16 weeks of age) SDT fatty rats. In addition, in order to verify the possibility of using these animals as a DPN model, we investigated the effects of glycemic control on DPN using the anti-diabetic drug phlorizin.

The results of the present study showed that male SDT fatty rats experienced significant decreases in SNCV, a tendency for decreases in MNCV and IENFD, and morphological abnormalities in small myelinated and unmyelinated fibers of sural nerves by 16 weeks of age. Furthermore, a trend towards decreases in $CV_{R\text{-}R}$ was observed in the evaluation of autonomic nerve function. The nerve conduction velocity indicates the function of large-fiber neuropathy, while IENFD and $CV_{R\text{-}R}$ indicate small-fiber neuropathy (Sumner et al., 2003; Pittenger et al., 2004). Abnormalities of small myelinated fibers and unmyelinated fibers observed in TEM analyses of SDT fatty rats are thought to be related to decreases in IENFD and $CV_{R\text{-}R}$. Although only a slight influence on large diameter myelinated fibers was observed in TEM analyses, the delay of SNCV and MNCV in SDT fatty rats is thought to indicate large-fiber

neuropathy. The occurrence of functional abnormalities, such as decreases in NCV and $CV_{R\text{-}R}$, were associated with histopathological changes. As morphological abnormalities in the DPN model animals, the thinning of myelin (Chen et al., 2016) was also observed in this study, and axonal atrophy, demyelination and myelin degeneration in STZ-induced diabetic rats (Chen et al., 2016; Sameni and Panahi, 2011; Yu et al., 2006) and demyelination in Goto-Kakizaki (GK) rats (Wada et al., 1999) have been reported. The main findings in this study included mitochondrial abnormalities in small myelinated and unmyelinated fibers. In an in vitro evaluation using dorsal root ganglion neurons, a hyperglycemic state reportedly caused apoptosis and mitochondrial swelling, suggesting a link between hyperglycemia and neuropathy (Vincent and Feldman, 2004). Therefore, mitochondrial abnormalities in the sural nerves of SDT fatty rats suggest that hyperglycemic conditions are involved in DPN.

In clinical practice, IENFD is highly variable in the early stages of DPN, and apparent decreases in IENFD are observed during the late stage, resulting in IENFD being an indicator of the progression of neuropathy (Arimura et al., 2013). From the results of IENFD in SDT fatty rats at 16 weeks of age, the pathological condition was considered as being possibly correlated to the early stage of clinical presentation. According to the previous report (Yamaguchi et al., 2012), the number of sural nerve fibers tended to be reduced in SDT fatty rats at 24 weeks of age, but a significant reduction was not observed until 40 weeks of age. Considering this result, it is considered that the present finding is reasonable, and in order to obtain the obvious changes, it is necessary to be evaluated in the aged rats.

Male SDT fatty rats also showed elevated blood pressure, similar to results in the previous report (Ishii et al., 2010b). The increase in blood pressure in SDT fatty rats

was reportedly caused by metabolic disorders, such as hyperglycemia and hyperlipidemia. In this study, significant reductions in SBP were observed with the improvements of hyperglycemia and hyperlipidemia in phlorizin-treated SDT fatty rats. These results suggest that the increase in blood pressure in SDT fatty rats is related with glucose/lipid metabolic abnormalities. The body weights and plasma insulin levels of the phlorizin-treated group were higher than those of the vehicle-treated (control) groups. The increase in plasma insulin levels may be induced by an improvement of pancreatic function with the good glycemic control. Furthermore, it is considered that the improvement of glucose metabolic abnormalities and the increase in plasma insulin levels lead to the increase in body weight.

Miosis and reduced reactivity to mydriatic drops were observed in male SDT fatty rats. Diabetic patients reportedly have small pupil diameters (Rickmann et al., 2016; Karavanaki et al., 1994) and responsiveness to mydriatic agents was lower in DM patients than in healthy subjects (Huber et al., 1985). Pupil abnormalities in DM patients are thought to be based on autonomic nervous disorders (Sigsbee et al., 1974), suggesting that the response observed in this study indicates autonomic dysfunction in male SDT fatty rats.

Autonomic abnormalities in adult DM patients in the early stages of neuropathy improved with glycemic control (Jakobsen et al., 1988). In this study, improvements in $CV_{R\text{-}R}$, blood pressure and pupillary reactivity were observed with phlorizin treatment, suggesting that hyperglycemia is involved in the autonomic dysfunction of male SDT fatty rats. We hypothesized that this rat showed autonomic dysfunction, as well as abnormalities in sensory and motor nerves at an early age at 16 weeks of age. The onset of DPN in animal models is often observed later, once the

animals are older. For example, Tsumura Suzuki Obese Diabetes (TSOD) mice develop motor neuropathy after 14 months of diabetes (Iizuka et al., 2005), and GK rats present with conduction velocity delays and structural abnormalities, such as axonal degeneration, starting from 18 months of age (Murakawa et al., 2002). Decreases in $CV_{R\text{-}R}$ were also reported in sucrose-fed Otsuka Long-Evans Tokushima Fatty (OLETF) rats at 35 weeks of age (Nakamura et al., 2001). Even compared with other diabetic animal models, the male SDT fatty rat develops DPN of sensory/motor nerves and autonomic nerves at a very early stage. The evaluation using responses to mydriatic agents utilized in this study was suggested as being a useful index for autonomic nerve function evaluations similar to $CV_{R\text{-}R}$.

Risk factors involved in the onset and progression of diabetic neuropathy include poor glycemic control, time from onset of DM, hypertension, and lipid abnormality (Tesfaye et al., 2005). The most important factor is poor glycemic control, and patients presenting with these symptoms frequently develop DPN (Partanen et al., 1995). Numerous other diabetic animal models are not validated with anti-diabetic drugs or antineuropathic drugs (Islam, 2013). In type 2 DM animal models, DPN observed in *ob/ob* mice improved with fidalrestat treatment, which is an aldose reductase inhibitor (Drel et al., 2006), and glycemic control was achieved with the use of voglibose, an α-glycosidase inhibitor. MNCV and nerve demyelination also improved in GK rats (Wada et al., 1999). In the type 1 DM model, STZ-induced neuropathies improved with increased glycemic control caused by insulin treatment in rats (Filho and Fazan, 2006) and mice (Murakami et al., 2013). The male SDT fatty rat, an obese diabetic model, is considered to be useful for drug discovery research in the DPN area.

In this study, some parameters related to DPN were measured in SDT fatty rats

and, MNCV, IENFD and $CV_{R\text{-}R}$ were failed to reach statistical significance. In the evaluation using SDT fatty rats, it is considered that SNCV is useful as peripheral nerve evaluation, blood pressure and responsiveness to mydriatic agents are useful as autonomic nerve evaluation at an early stage. On the other hand, MNCV, IENFD and $CV_{R\text{-}R}$, which did not have significant difference, could be positioned as supplemental data at an early stage. It is necessary to be evaluated in the long-term and/or to increase the number of animals to be evaluated. In the TEM analysis, mitochondrial degeneration was observed, and it is also necessary to evaluate the changes in the aged rats.

In conclusion, male SDT fatty rats may be useful model in future work on DPN in type 2 DM, because male SDT fatty rats exhibit morphological and functional abnormalities in the somatic and autonomic nerves dependent on hyperglycemia at an early stage.

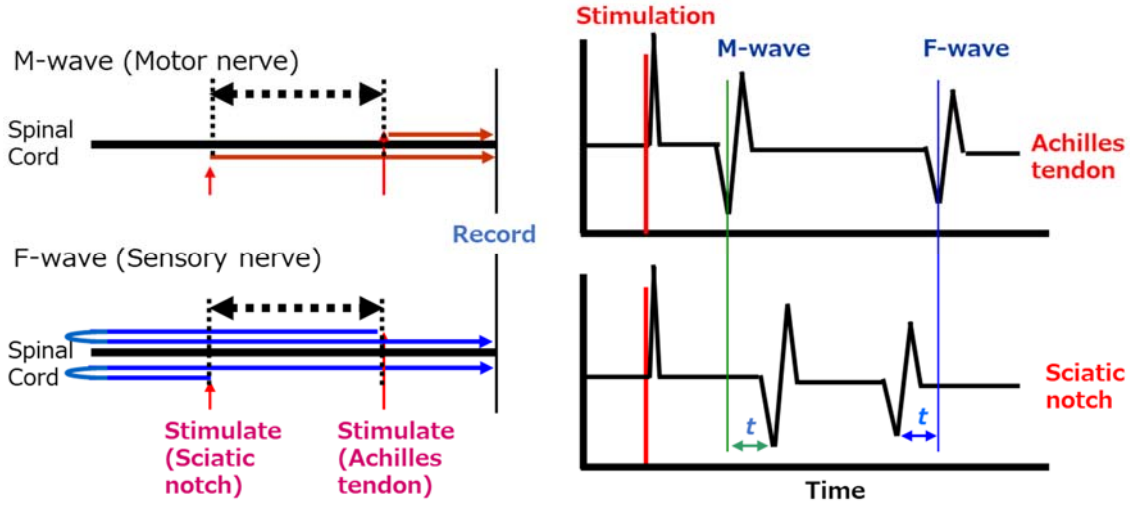

Figure 1 Measurement method of sciatic nerve conduction velocity.

SNCV (m/sec) = distance between the sciatic nerve and Achilles tendon (mm) / (peak latency of an F-wave in the Achilles tendon – peak latency of an F-wave in the sciatic notch) (msec)

MNCV (m/sec) = distance between the sciatic nerve and Achilles tendon (mm) / (peak latency of an M-wave in the sciatic notch – peak latency of an M-wave in the Achilles tendon) (msec)

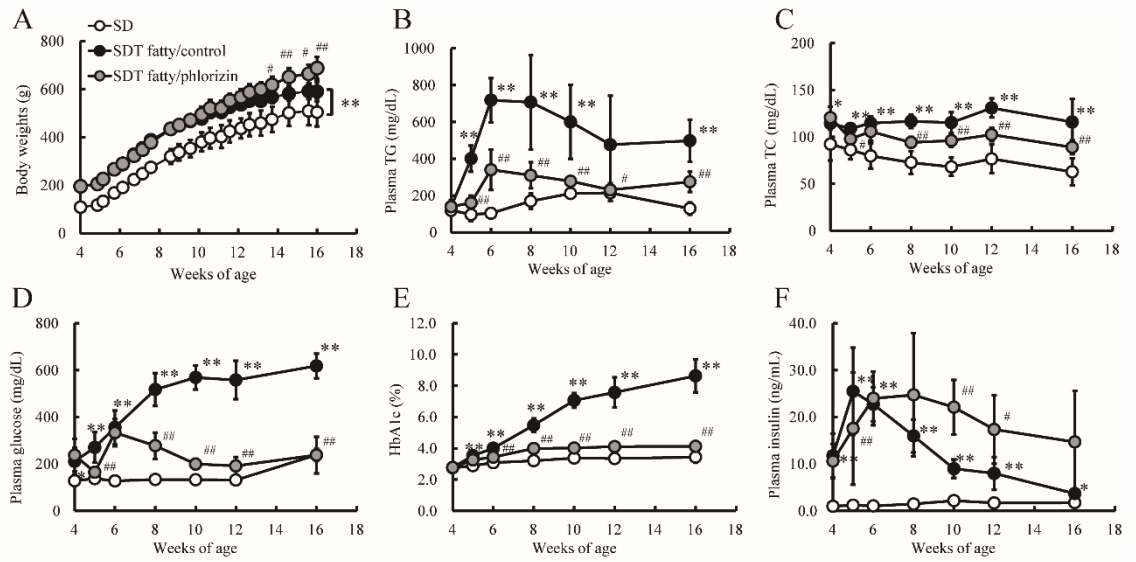

Figure 2 Changes in biochemical parameters of SDT fatty rats. Changes in body weight (A), plasma triglyceride levels (B), plasma total cholesterol levels (C), plasma glucose levels (D), blood HbA1c levels (E), and plasma insulin levels (F). White circles = SD rats (normal); black circles = SDT fatty rats (control); gray circles = SDT fatty rats (phlorizin). Each value represents the mean ± standard deviation (n=6). *p<0.05, **p<0.01 vs. SD rats (normal). #p<0.05, ##p<0.01 vs. SDT fatty rats (control) (Two-way ANOVA with Student's or Aspin-Welch's *t*-test).

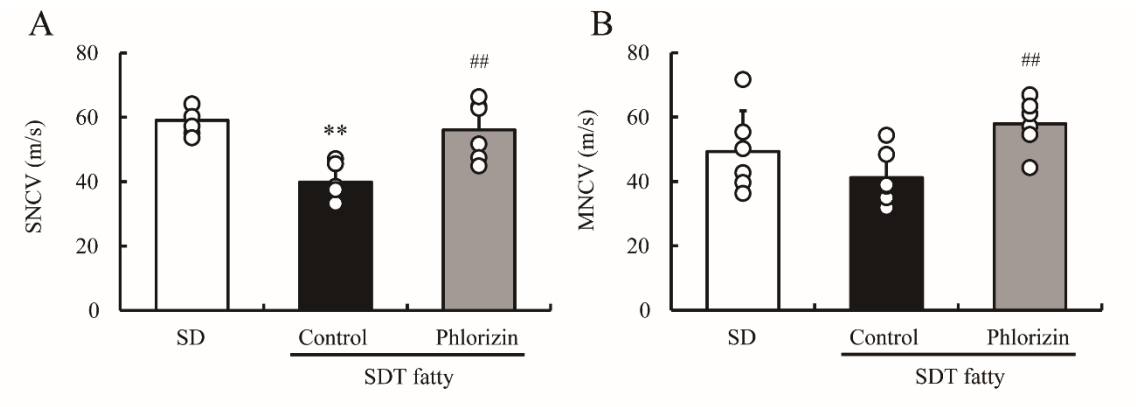

Figure 3 Assessment of sciatic nerve conduction velocity in SDT fatty rats. Sensory nerve conduction velocity (A), and motor nerve conduction velocity (B) of the sciatic nerve were measured at 15 weeks of age. Each value represents the mean ± standard deviation (n=6). **p<0.01 vs. SD rats (normal). #p<0.05 vs. SDT fatty rats (control) (One-way ANOVA with Student's or Aspin-Welch *t*-test).

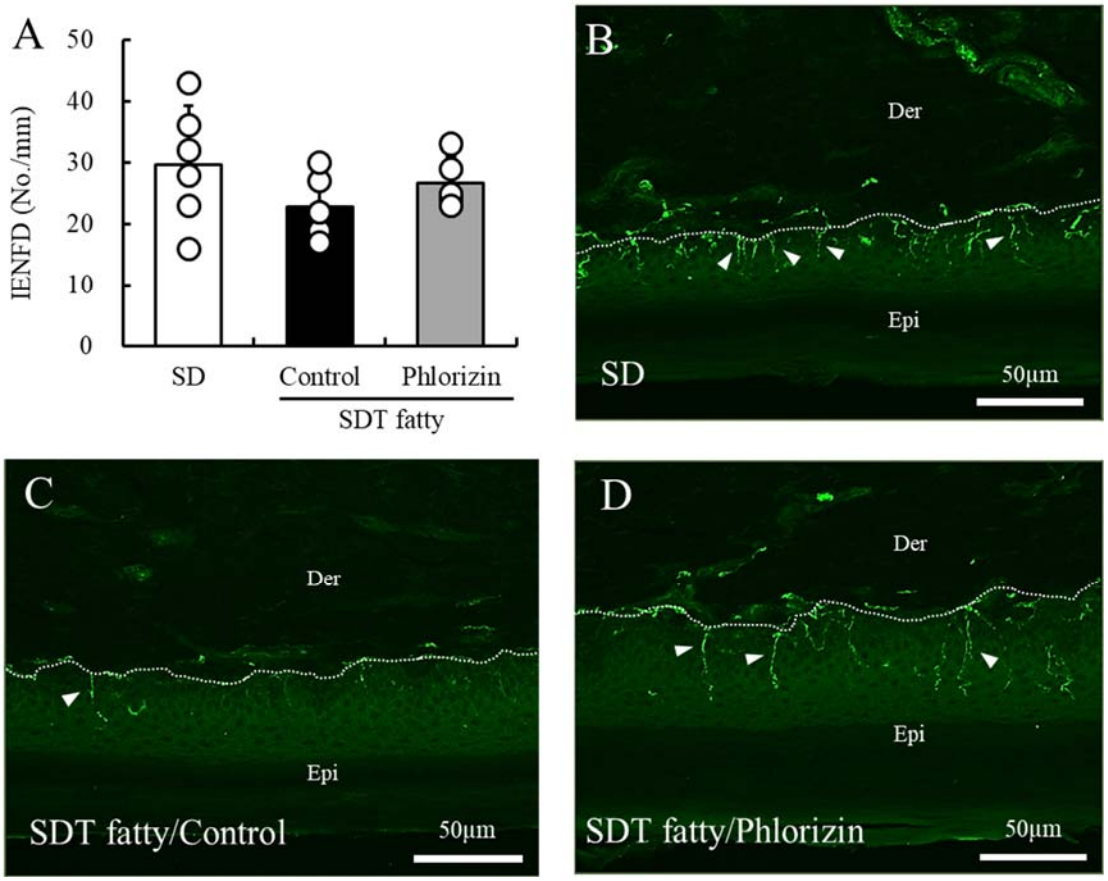

Figure 4 Intraepidermal nerve fiber density (IENFD) in SDT fatty rats. The density of nerve fibers (A) was measured at 16 weeks of age. Values represent the mean ± standard deviation (n=5 to 6). Panels B to D show PGP 9.5 immunoreactive epidermal nerve fibers (green) in SD rats (normal, B), SDT fatty rats (control, C), and SDT fatty rats (phlorizin, D), respectively. Epi: Epidermis, Der: Dermis, dotted line: dermoepidermal junction. Arrow heads indicate the example of the intraepidermal nerve fiber. Scale bar = 50 μm.

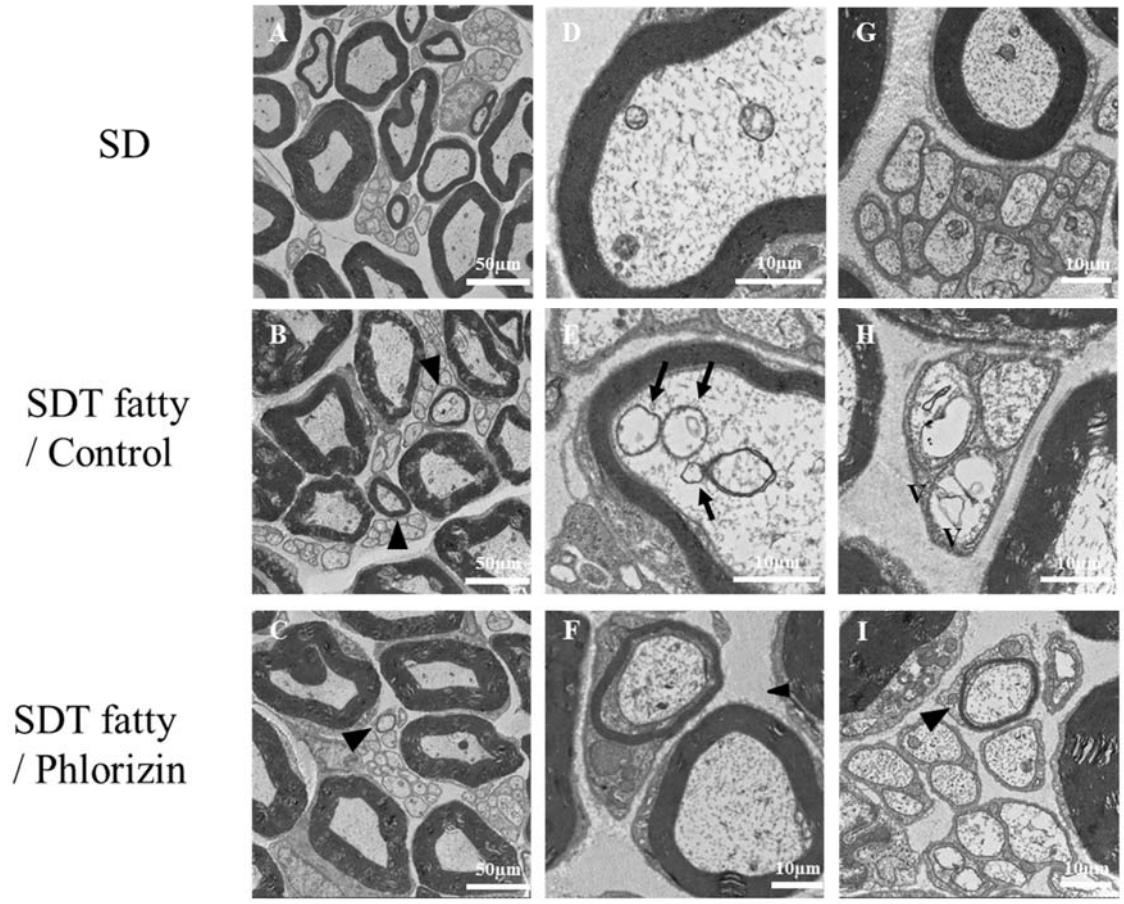

Figure 5 Representative electron micrographs of sciatic nerves of SDT fatty rats. Arrow heads indicate the thinning of myelin sheaths, and arrows indicate mitochondrial abnormalities in myelinated nerve fibers. Panel H indicates unmyelinated fibers with vacuolation (V). Scale bar = 50 μm (A to C), 10 μm (D to I).

Table 1

Morphological changes in myelinated and unmyelinated fibers.

Strain	SD	SDT fatty	
Group	Normal	Control	Phlorizin
Number of Animals	6	6	6
Large myelinated fibers			
Vacuolation	0/6	1/6	0/6
Small myelinated fibers			
Mitochondrial abnormalities [a]	0/6	3/6	0/6
Thinning of the myelin sheath	0/6	6/6	6/6
Vacuolation	0/6	1/6	1/6
Unmyelinated fibers			
Vacuolation	0/6	4/6	1/6
Mitochondrial swelling	0/6	4/6	2/6

a Mitochondrial abnormalities in small myelinated fibers indicate the swelling or degeneration of mitochondria.

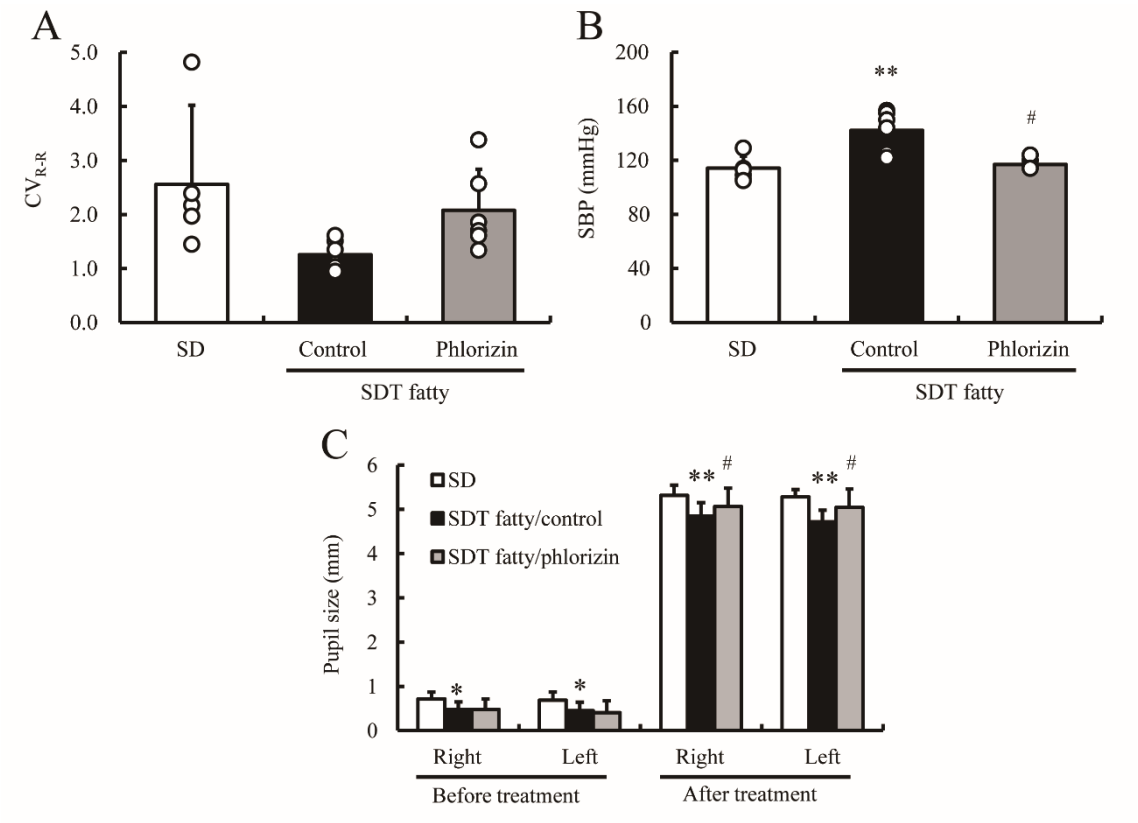

Figure 6 Assessment of the autonomic nerve function of SDT fatty rats. The coefficient of variance of R-R intervals (A), systolic blood pressure (B), and pupil size before and after the instillation of mydriatic drops (C) were measured at 15 weeks of age. Each value represents the mean ± standard deviation (n=6). **p<0.01 vs. SD rats (normal). #p<0.05 vs. SDT fatty rats (control) (One-way ANOVA with Student's or Aspin-Welch's *t*-test).

Chapter 3

Pathophysiological abnormalities in the brains of Spontaneously Diabetic Torii-*Lepr*^{fa} (SDT fatty) rats, a novel type 2 diabetic model

INTRODUCTION

There is some evidence of a relationship between DM and neurodegenerative diseases, such as Parkinson's disease (Hu et al., 2007), AD (Li et al., 2015), depression (Anderson et al., 2001) or cognitive dysfunction (Strachan et al., 1997), in patients. Diabetes-related cognitive dysfunction is complicatedly intertwined with long-term hyperglycemia, insulin deficiency and genetic/environmental factors (Stranahan, 2015) and is also associated with increased risk of dementia and AD (Yates et al., 2012). Although the mechanism by which DM reduces cognitive function is not clear, several factors such as oxidative stress, neuroinflammation, and neuronal apoptosis have been shown to be involved in the impairment of brain structure and function (Wrighten et al., 2009; Stranahan, 2015).

In AD patients, a typical neurodegenerative disease, cognitive decline, and morphological abnormalities such as cerebral atrophy and cell death have also been reported from Magnetic Resonance Imaging (MRI) and postmortem brain studies (Frolich et al., 1998; Moran et al., 2015). Cortical volume and cortical thickness have also been reported as being decreased in type 2 DM patients without AD (den Heijer et al., 2003; Brundel et al., 2010). Furthermore, in preclinical studies, AD pathogenesis, cognitive decline, and morphological abnormalities in the brain have been reported in

diabetic model animals. For example, forebrain cortex and hippocampal volume reduction, neurodegeneration, and increases in Aβ42 have been observed in STZ-induced diabetic rats (Wang et al., 2014). Impairments in both maze performance and hippocampal long-term potentiation (LTP) have been observed in OLETF and Zucker Diabetic Fatty (ZDF) rats (Nomoto et al., 1999; Belanger et al., 2004). Many clinical and preclinical studies suggest that diabetes is closely related to cognitive dysfunction such as AD.

SDT fatty rats have been reported to be a useful animal model for investigating diabetic complications associated with DM in the kidneys, eyes, and peripheral nerves (Matsui et al., 2008; Ishii et al., 2010a: Katsuda et al., 2015; Maekawa et al., 2017). In addition, SDT fatty rats have also been shown to be a feasible model for depression (Sakimura et al., 2018). Since diabetes is observed from a young age in this model, the expectation is that the animals may exhibit neurodegenerative diseases that are found in other diabetic model animals. However, there have been no reports to date on neurodegenerative diseases of the brain in this model. In this study, we investigated the pathophysiological changes in the brains of male SDT fatty rats.

MATERIALS AND METHODS

Animals

This experiment was conducted in strict compliance with our own Laboratory Guidelines for Animal Experimentation and was approved by the Institutional Animal Care and Use Committee of Central Pharmaceutical Research Institute of Japan Tobacco Inc. A total of 15 male SDT $^{fa/fa}$ (SDT fatty) rats (Clea Japan, Tokyo, Japan) were used in the study. Fifteen age-matched male SD rats (Clea Japan) were used as control

animals. Animals were housed in a climate-controlled room (temperature 23 ± 3°C, humidity 55 ± 15%, 12hr lighting cycle) and allowed free access to a basal diet (CRF-1, Oriental Yeast, Tokyo, Japan) and sterilized water.

Measurement of Biophysiological Parameters

Body weights and biochemical parameters, such as plasma glucose, insulin, and blood HbA1c, were measured at 32 and 58 weeks of age in a non-fasting state. Blood samples were collected from the subclavian vein of rats. Plasma glucose, and blood HbA1c were measured using commercial kits (Roche Diagnostics, Basel, Switzerland) and an automatic analyzer (HITACHI Clinical analyzer 7180; Hitachi, Tokyo, Japan). Plasma insulin levels were measured using rat insulin ELISA kits (Morinaga Institute of Biological Science, Yokohama, Japan).

Tissue Sampling

Necropsies were conducted at 32 and 58 weeks of age and brains were collected from all animals. For the histopathological examination, rats were anesthetized with isoflurane, and then subjected to transcardiac perfusion with 0.1M Phosphate buffered saline (PBS) and 4% paraformaldehyde. For the mRNA analysis, designated rats at 58 weeks of age were also subjected to transcardiac perfusion with 0.1M PBS under isoflurane anesthesia, and brain samples were stored at -80°C until analysis.

Morphometric Examination

The tissues were paraffin-embedded using standard techniques and were thin-sectioned (5 μm) from approximately −3.30 mm from the bregma. The sections

were stained with hematoxylin and eosin (HE) and Nissl. Each stained section was photographed under an optical microscope and images were digitally saved. HE-stained sections were used to measure left and right parietal cortical thicknesses, and left and right mean values were calculated. Nissl stained sections were used to measure pyramidal cells in the left and right hippocampal cornu ammonis 1 and 3 (CA1 and CA3) regions. Using image processing software, Image J (National Institute of Health, USA), the number of pyramidal cells in each of the 3 left and right locations (6 locations in total) per unit area was measured for each section using a blinded method. The unit area was set to 50 × 150 μm for both the CA1 and CA3 regions of the hippocampus. The number of pyramidal cells was taken as the average value of 6-unit areas. In this experiment, only cells with clear nuclear borders and boundaries were counted.

Amyloid Staining

Paraffin sections were deparaffinized with xylene, rehydrated in graded (100, 95 and 90%) ethanol (EtOH) and washed with distilled water. For BSB staining, sections were incubated with 0.01% BSB (1-Bromo-2,5-bis(3-carboxy-4-hydroxystyryl)benzene, Dojindo Molecular Technologies, Inc., Japan) solution in 50% EtOH for 30 min. Sections were differentiated in saturated lithium carbonate and rinsed in 50% EtOH before examination by fluorescent microscopy. For immunohistochemistry staining, sections were incubated with 99% formic acid at room temperature for 30 minutes, and then with citrate buffer at 95ºC for 30 minutes. After being rinsed with PBS, sections were quenched in 0.3% H_2O_2 at room temperature for 30 minutes. Sections were blocked with normal goat serum at room temperature for 20

minutes, and incubated overnight at 4ºC with rabbit polyclonal $A\beta_{1\text{-}40}$ and $A\beta_{1\text{-}42}$ ($A\beta_{1\text{-}42}$) antibodies (Immuno-Biological Laboratories Co, Ltd., Gunma, Japan). The sections were then incubated with the respective biotinylated secondary antibodies at room temperature for 30 minutes. The brain slices were further incubated in ABC reagent (Vectastain Elite ABC Kit, Vector Laboratories, CA, USA) at room temperature for 30 minutes. The reaction was revealed by incubating the sections with ImmPACT™ DAB (diaminobenzidine; Vector Laboratories, CA, USA). Sections were dehydrated in ascending (90, 95 and 100%) EtOH, followed by immersion in xylene, and then sealed with a water-insoluble encapsulant (Nichirei Bioscience Inc., Tokyo, Japan).

mRNA from Real-Time Reverse-Transcriptase-Polymerase Chain Reaction

Total RNA was extracted from the brains at 58 weeks of age using the miRNeasy Mini Kit (Qiagen, Hilden, Germany) according to the manufacturer's protocols. Complementary DNA (cDNA) was synthesized from 1 μg of total RNA using a High-Capacity cDNA Reverse Transcription Kit with an RNase Inhibitor (Applied Biosystems, Foster City, CA, U.S.A.). The reaction mixture was incubated for 10 min at 25°C, 2 hrs at 37°C, and 5 min at 85°C. Real-time polymerase chain reaction (PCR) quantification was performed in a 10 μL reaction mixture on a QuantStudio 7 Real-Time PCR system (Applied Biosystems). The reaction mixture contained 1× TaqMan Universal PCR Master Mix II (Applied Biosystems), 20 ng of synthesized cDNA, and 0.9 μM primers/0.25 μM probes or TaqMan primers/probe mix (TaqMan Gene Expression Assays, Applied Biosystems). Cycle parameters were 10 min at 95°C, followed by 40 cycles of 15 sec at 95°C and 1 min at 60°C. The expression of the following genes was confirmed using TaqMan Gene Expression Assays: β-actin

(Rn00667869_m1), S100 calcium binding protein A9 (S100a9) (Rn00585879_m1), heat shock 70kD protein 1A (HSP70-1a) (Rn04224718_u1), nuclear factor of kappa light polypeptide gene enhancer in B-cells (NF-κB) (Rn01399572_m1), and tumor necrosis factor (TNF)-α (Rn99999017_m1). Each relative change in gene expression level was calculated using the $2^{-\Delta\Delta Ct}$ method (Livak and Schmittgen, 2001).

Statistical Analysis

Results were expressed as means ± standard deviations. Statistical analyses of differences between mean values in SD rats and SDT fatty rats were performed using the F-test, followed by Student's *t*-test or Aspin-Welch's *t*-test. Differences were defined as significant when $p < 0.05$.

RESULTS

Body Weights and Biophysiological Parameters

The body weights of SDT fatty rats were significantly ($p<0.01$) lower than those of age-matched SD rats at 32 and 58 weeks of age (Figure 7A). The plasma glucose levels and blood HbA1c levels of SDT fatty rats were obviously higher than that of SD rats at both ages (Figures 7B and 7C). The fluctuations in HbA1c levels reflected the changes in blood glucose levels. The plasma insulin levels of SDT fatty rats were significantly ($p<0.01$) lower than those of SD rats after 32 weeks of age (Figure 7D).

Morphometric Analysis

The parietal cortical thickness of SDT fatty rats was significantly ($p<0.05$)

lower than that of age-matched SD rats at 58 weeks of age, but not at 32 weeks of age (Figure 8). At 58 weeks of age, the thickness in SD rats and SDT fatty rats was 1.05 ± 0.08 mm (n = 5) and 0.94 ± 0.04 mm (n = 5), respectively. The number of cells in the CA1 and CA3 regions of the hippocampus of SDT fatty rats was significantly ($p<0.01$) lower than that of age-matched SD rats at 58 weeks of age, but not at 32 weeks of age (Figure 9 and 10). The number of pyramidal cells in the CA1 region was 27.4 ± 1.4 in SD rats (n = 5) and 22.3 ± 1.1 in SDT fatty rats (n = 5) at 58 weeks of age. The number in the CA3 region was 21.0 ± 0.4 in SD rats (n = 5) and 16.6 ± 1.4 in SDT fatty rats (n = 5) at 58 weeks of age.

Amyloid Staining

In experiments using BSB staining and Aβ staining, no amyloid-positive sites were observed in brain sections of SDT fatty rat (Figure 11).

mRNA Analysis

Changes in mRNA expression related to inflammation in the brain at 58 weeks of age were determined for each group. In the brain of SDT fatty rats (n = 4), the mRNA expression of S100a9, a calcium binding protein, and TNF-α, a cytokine involved in inflammation and NF-κB, a transcription factor, in the brain significantly ($p<0.01$, 0.01 and 0.05, respectively) increased compared with those in SD rats (n = 5), and the mRNA expression of HSP70-1a, a molecular chaperone, tended to increase (Figure 12).

DISCUSSION

In the present study, the morphological changes in the brains of SDT fatty rats

that developed obesity and diabetes were investigated. The parietal cortical thickness and hippocampal pyramidal cells in the CA1 and CA3 regions decreased in SDT fatty rats. The relationship between cerebral cortical thickness and DM has been reported in clinical practice and animal models. Diabetic patients have been reported to have a cerebral cortex thickness of 0.03 mm, which is lower than the thickness observed in those without DM regardless of cognitive impairment (Moran et al., 2015). Similarly, in *db/db* mice in a T2DM model, reductions in cortical thickness have been reported compared with control (Ramos-Rodriguez et al., 2014). Therefore, the decrease in cortical thickness observed in SDT fatty rats in this study is considered to contribute to the hyperglycemic state. In addition, Moran et al. mentioned that "cortical atrophy in T2DM is similar to that seen in preclinical AD, and neurodegeneration may play a key role in cognitive deficits associated with T2DM" (Moran et al., 2013). Therefore, changes in cortical thickness in SDT fatty rats are suggested as being a possible change related to cognitive impairment. The number of pyramidal cells in the hippocampal CA1 and CA3 regions was low in SDT fatty rats. The CA1 region of the hippocampus is reportedly a site in which CA1 neuronal density volume is reduced in patients with dementia and AD post-stroke, or ischemic vascular disease (Gemmell et al., 2012). Furthermore, the CA3 region is reportedly weak against aging, and the number of cells per unit area decreases due to aging (Tanaka et al., 1995). Reductions in nerve density in the hippocampal region of BB/W rats in a type 1 DM model (Li et al., 2002) and reductions in nerve density of the prefrontal cortex in BBZDR/Wor rats in a T2DM model (Li et al., 2007) have been reported. In this study, the number of pyramidal cells in the hippocampus did not change with age in SD rats; however, SDT fatty rats showed a decrease in the number of pyramidal cells. This result suggests that the sustained

hyperglycemia may contribute to these morphological changes. In the preliminary study, the brain weights of SDT fatty rats at 32 and 58 weeks of age were measured. At 32 weeks of age, the absolute brain weights decreased, and the relative brain weights increased in SDT fatty rats (absolute weights; 2,031 ± 63 mg, relative weights; 4.2 ± 0.5 mg/g body weight) as compared with the age-matched SD rats (absolute weights; 2,233 ± 49 mg, relative weights; 2.8 ± 0.3 mg/g body weight). Changes in the brain weights at 58 weeks of age (SD rats: absolute weights; 2,251 ± 87 mg, relative weights; 2.2 ± 0.3 mg/g body weight, SDT fatty rats: absolute weights; 2,033 ± 56 mg, relative weights; 5.0 ± 0.4 mg/g body weight) were similar to those at 32 weeks of age. Since changes in the brain weights were observed before the morphological changes occurred, it is necessary to investigate the relationship between the brain weights and the pathophysiological changes in other brain regions.

Intracerebral amyloid deposition has been reported in Tg2576 transgenic mice and STZ-treated human APP transgenic mice (Skovronsky et al., 2000; Horikoshi et al., 2004; Jolivalt et al., 2010). BSB has high affinity for Aβ peptide (Skovronsky et al., 2000). However, amyloid deposits were not observed in brains of SDT fatty rats. This suggested that brain morphological abnormality of SDT fatty rats at 58 weeks of age may be amyloid-independent changes.

In the present study, the expression of inflammation-related genes was observed in the brains of SDT fatty rats. S100a9 reportedly participates in the inflammation of AD pathogenesis (Shepherd et al., 2006). Furthermore, the expression of S100a9 is also recognized in AD patients and in genetically modified AD animal models, and the expression of S100a9 is suggested as possibly being involved in AD pathology (Ha et al., 2010). Neuroinflammation is known as a crucial factor in the mechanism that

associates T2DM with AD. Increased interleukin-1 and TNF-α mRNA in the hippocampus of *db/db* mice (Dinel et al., 2011) and TNF-α may elicit insulin resistance in the hippocampus (Bomfim et al., 2012), and increased expression of NF-κB that promotes the production of inflammatory cytokines in the brain of high-fat diet and STZ-induced diabetic mice (Pahl, 1999; Jiang et al., 2012) were reported. In addition, the upregulation of S100a9 has been reported to activate the p38 mitogen-activated protein kinase cascade and NF-κB (Hermani et al., 2006). Therefore, neuroinflammation was considered as being involved in the brain abnormality observed in this model. It has been reported that HSP70-1a is induced by various stress and it has anti-inflammatory and cytoprotective effects (Daugaard et al., 2007; Matsuda et al., 2010). On the other hand, lipopolysaccharides, which induce inflammation, reportedly induced HSP70-1a expression (Mansilla et al., 2014). Since SDT fatty rat is a hyperglycemic and obese model, it may be exposed to chronic inflammation and stress by those factors. In this study, HSP70-1a tended to be increased in the brains of SDT fatty rats, suggesting the involvement of inflammation and stress.

It has been reported that insulin resistance, AGEs, oxidative stress and inflammatory response are involved in cognitive dysfunction of human DM patients (Muriach et al., 2014). SDT fatty rats have also been reported to represent insulin resistance and inflammatory responses (Ishii et al., 2015). Elevated expression of inflammation-related gene has also been observed in this study, and neuroinflammation with the sustained hyperglycemia may cause organic changes in the brain. In addition, female SDT fatty rats represent an obvious hyperinsulinemia as compared with male SDT fatty rats (Ohta et al., 2014), and a severe insulin resistance may be induced in the brain of female SDT fatty rats. To investigate the pathophysiological changes in the

brain of female SDT fatty rats is worthful as a future plan.

In this study, histological analyses revealed that SDT fatty rats showed brain atrophy and a decreased number of hippocampal cells. The behavioral evaluation is often used in the evaluation of cognitive functions of animals (Ho et al., 2013). SDT fatty rats reportedly show a depression-like behavior (Sakimura et al., 2018) as one of behavioral features, and the evaluation of learning function is under consideration. Although the neurotransmitter such as serotonin, γ-aminobutyric acid and glutamate in the brain were impaired even in SDT fatty rats (Sakimura et al., 2018), histological changes in the brain developed in aged SDT fatty rats. Moreover, the survival rate of male SDT fatty rats at 50 weeks of age was approximately 70-80% in the preliminary study. From the viewpoint of versatility as a model animal, the early development of the brain pathological changes of SDT fatty rats is a future subject. In conclusion, this model rat showed the possibility of developing not only peripheral neuropathy (Maekawa et al., 2017) but also CNS disorders. The expectation is that this model can be used to elucidate the pathologic pathway in AD which is recently recognized as new type of DM (or type 3 DM) (de la Monte and Wands, 2008).

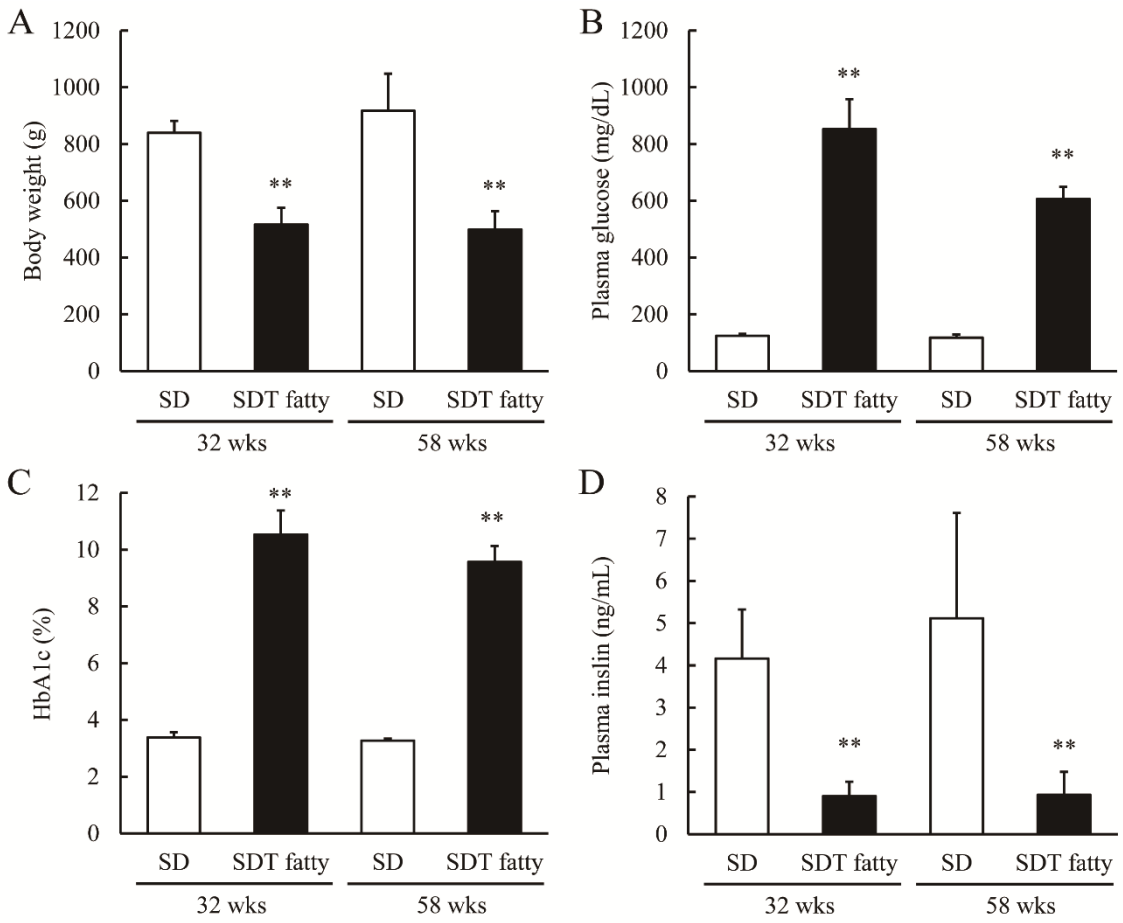

Figure 7 Changes in biochemical parameters in SDT fatty rats. Changes in body weight (A), plasma glucose levels (B), blood HbA1c levels (C), and plasma insulin levels (D). Data represent means ± standard deviations (n=5). **p<0.01; significantly different from the SD group.

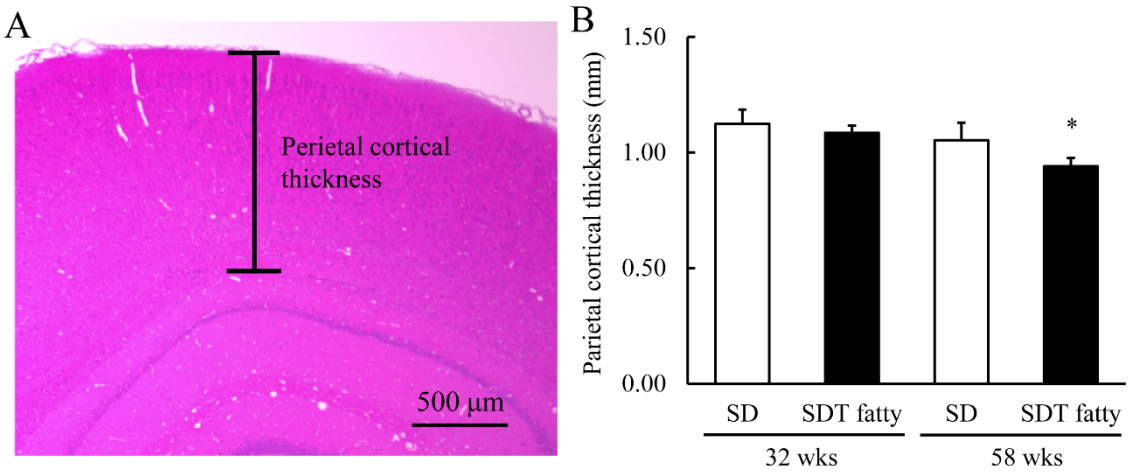

Figure 8 Brain atrophy in SDT fatty rats at 58 weeks of age. Illustrative example of cortical thickness (A). Thickness measurement of the parietal cortex in male SDT fatty rats at 32 and 58 weeks of age (B). Data represent means ± standard deviations (n=5). *p<0.05; significantly different from the age-matched SD group.

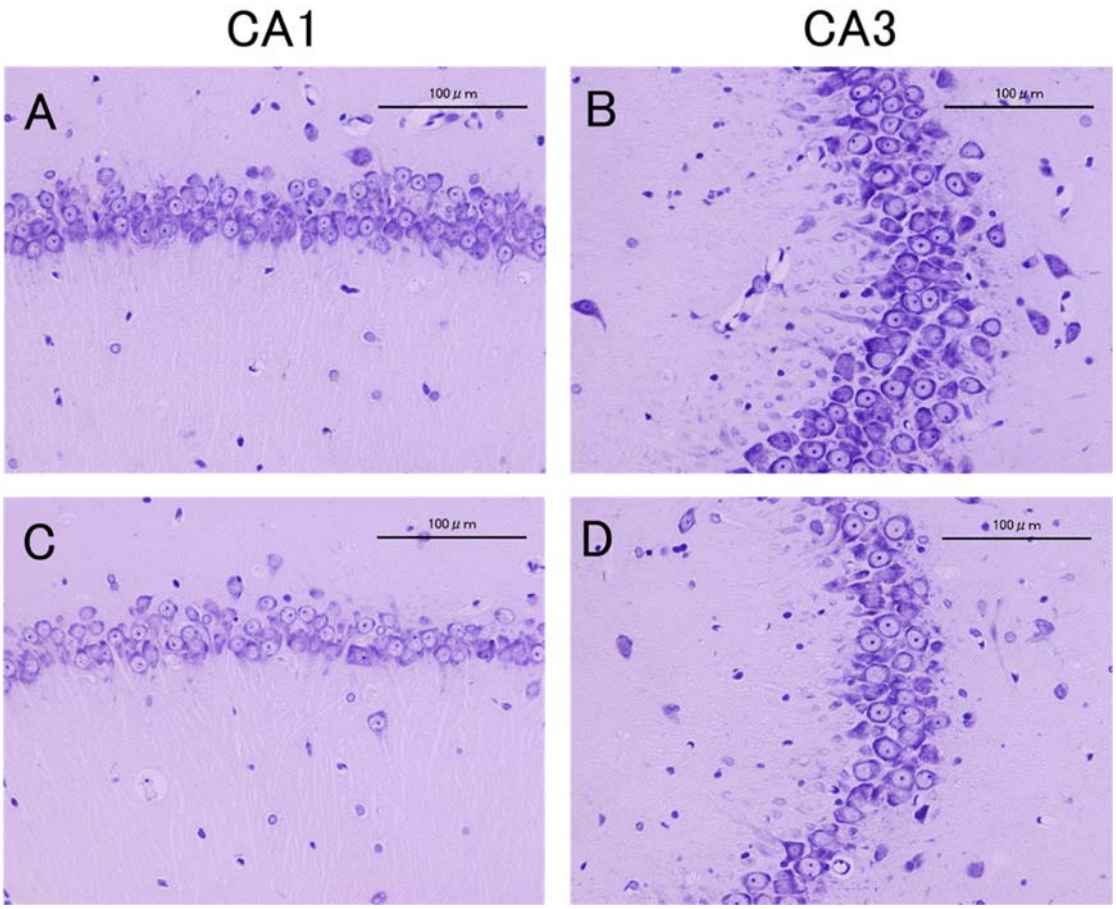

Figure 9 Illustrative example of the CA1 and CA3 regions in SD rats (A, B) and SDT fatty rats (C, D). Scale bar = 100 μm

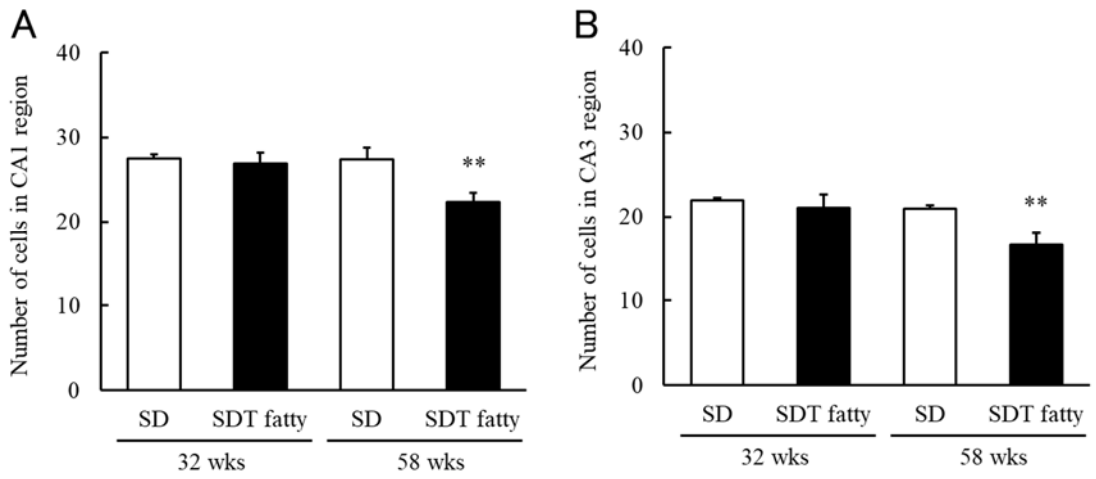

Figure 10 Number of cells in hippocampal CA1 and CA3 regions of SDT fatty rats at 32 and 58 weeks of age. Number of cells in the CA1 (A) and CA3 regions (B). Data represent means ± standard deviations (n=5). **p <0.01; significantly different from the age-matched SD group.

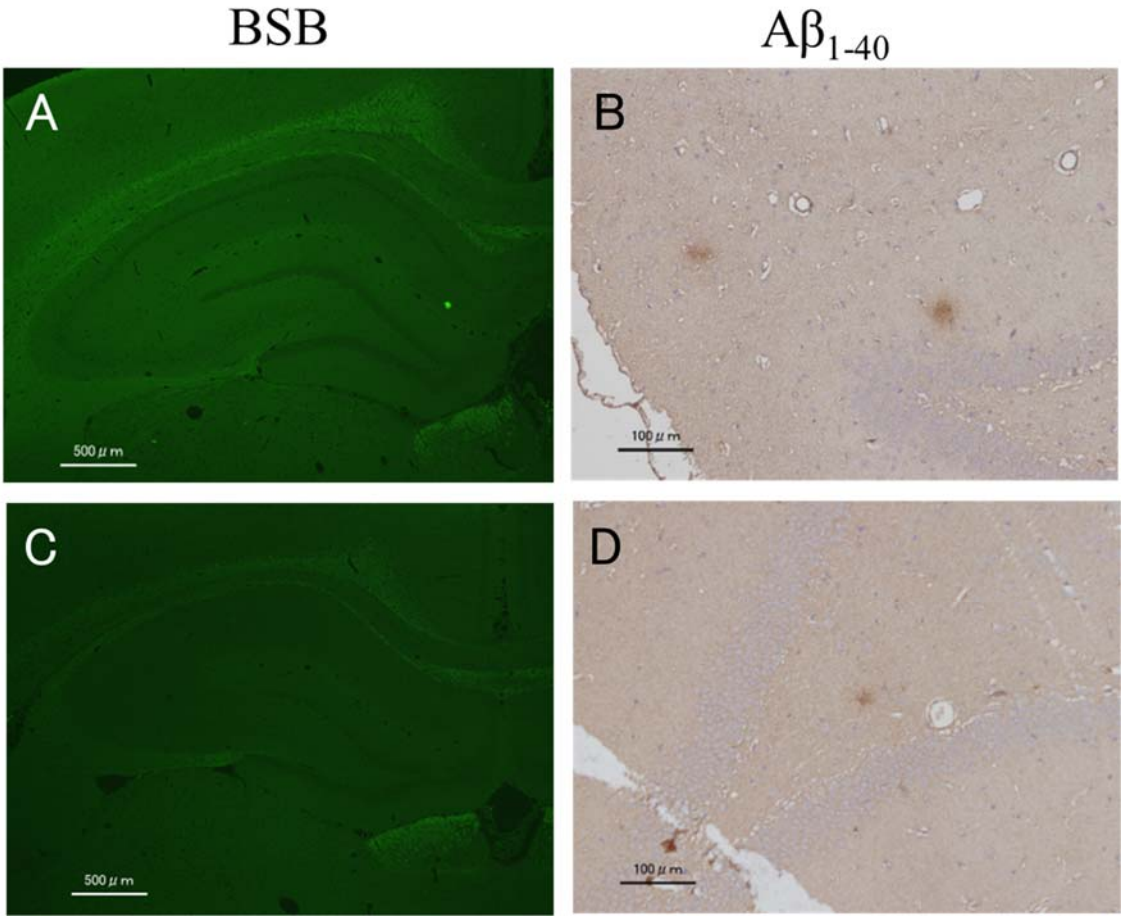

Figure 11 Illustrative example of the BSB fluorescent staining (A, C) and anti-amyloid $\beta_{1\text{-}40}$ staining (B, D) in SD rats (A, B) and SDT fatty rats (C, D). Scale bar = 100 μm.

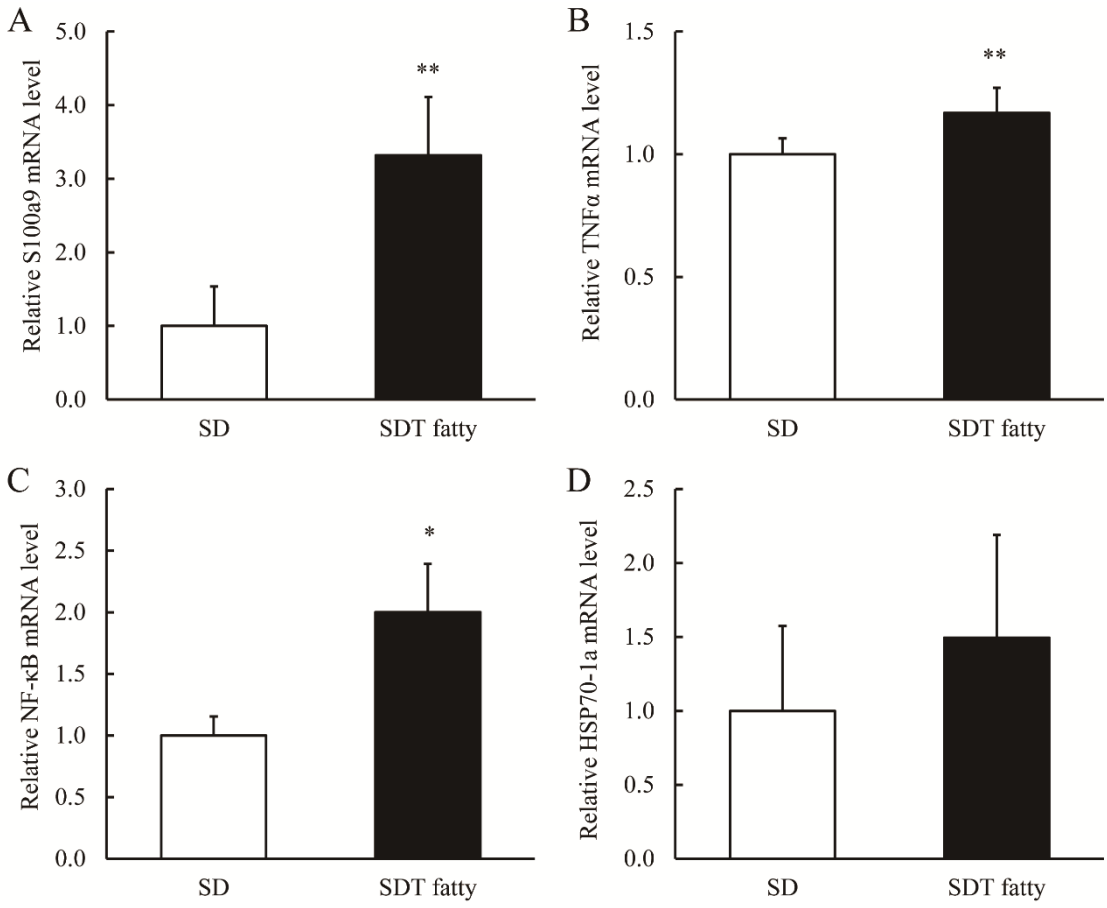

Figure 12 Changes in mRNA levels in SDT fatty rat brains at 58 weeks of age. Changes in S100a9 mRNA levels (A), TNF-α mRNA levels (B), NF-κB mRNA levels (C), and HSP70-1a mRNA levels (D). Data represent means ± standard deviations (n=4 to 5). *p<0.05, **p<0.01; significantly different from the SD group.

Chapter 4

General Discussion

Mechanism of Peripheral Neuropathy

DPN is defined as the presence of symptoms and/or signs of peripheral nerve dysfunction in people with DM, after the exclusion of other causes (Pop-Busui et al., 2017). DPN is a chronic complication that cannot be neglected, since it not only significantly impairs the patient's quality of life (QOL), but also has serious effects on the patient's life prognosis by causing severe foot gangrene or painless myocardial infarction. Basically, glycemic control is the first choice of treatment for DPN, but the development of a novel treatment for DPN is extremely important in the study of the pathological condition of the peripheral nerves in diabetic animal models.

SDT fatty rat is an obese type 2 DM model, and shows signs of DPN at 40 weeks of age (Yamaguchi et al., 2012). However, studies on the pathogenesis and mechanism of the development and progression of DPN, including early onset and drug responsiveness, in SDT fatty rats have not been performed in detail. Pathophysiological analysis provides a useful means for development of new therapies and clarification of pathology. Therefore, in Chapter 2, the mechanism of DPN was investigated using SDT fatty rats.

In the animal models, as a method for evaluating the peripheral nerve function, measurement of the nerve conduction velocity of the tail nerve and the sciatic nerve is used in most cases. Significant decrease in sensory nerve conduction velocity was observed in SDT fatty rats at 15 weeks of age, while the MNCV only tended to decrease (Chapter 2: Figure 3). Decrease in the conduction velocity of sensory nerve, but not

motor nerve, was observed in SDT fatty rats at 10 weeks of age (Murai et al., 2017). Considering that the dysfunction of the sensory nerve precedes in the clinical practice (Ogawa et al., 2006), there is a possibility of the onset stage of neuropathy at 15 weeks of age, while the conduction velocity of the motor nerve is not clearly decreased. On the other hand, although measurement of $CV_{R\text{-}R}$, which is one of indices of autonomic nervous function, has been reported in STZ-treated animals, there are few such reports in type 2 diabetic model animals. For example, OLETF rats, which are type 2 diabetic model rats, have been reported to have decreased $CV_{R\text{-}R}$ at 35 weeks of age by sucrose feeding, but spontaneous reduction in $CV_{R\text{-}R}$ is not observed (Nakamura et al., 2001). Another type of diabetic model, GK rat, shows a decrease in $CV_{R\text{-}R}$, but this change was confirmed at 50 weeks of age (Han, 2017). SDT fatty rats showed miosis, as observed in patients with DM, and further decreased responsiveness to mydriatic agents, elevated blood pressure, and a tendency for decrease in $CV_{R\text{-}R}$ were observed (Chapter 2: Figure 6). These results revealed that SDT fatty rats developed functional abnormalities in both somatic nerves and autonomic nerves. In addition, the functional abnormalities in the somatic and autonomic nerves at an early stage is one of the features of SDT fatty rat as a DPN model.

In recent years, the distribution of IENFD as observed by skin biopsy is useful as an objective indicator of DPN (Kennedy et al., 1996; Shun et al., 2004). Genetically diabetic *db/db* mice showed a decrease in IENFD, and similar decreases were observed in skin samples from DM patients using similar detection methods (Gibran et al., 2002). Reduction of IENFD has also been reported in GK rats (Han, 2017). Histological examination is also an important method to elucidate the mechanism of DPN. For example, atrophy of unmyelinated fibers was observed in STZ-induced diabetic sensory

neuropathic ddY mouse model (Murakami et al., 2013). Spontaneously diabetic WBN/Kob rat model shows a structural demyelination and remyelination, showing axonal degeneration and dystrophy in the sciatic nerve and tibial nerve (Yagihashi et al., 1993). In the resent study, SDT fatty rats showed the trend of a decline in IENFD, thinning of myelin sheath and mitochondrial morphological abnormality in small myelinated fibers, and showed vacuolation in unmyelinated fibers (Chapter 2: Figure 4, Figure 5 and Table 1). In diabetes, mitochondrial dysfunction and oxidative stress increase with increased free radicals in hyperglycemic conditions. These factors are considered as the major pathophysiological causes of DPN (Saini et al., 2007; Kumar et al., 2007). Clinically, axonal degeneration such as axonal loss, depletion of axon vesicles, and vacuolization of both myelinated and unmyelinated nerve fibers has been reported in the sural nerve (Yagihashi and Matsunaga, 1979). In this study, some similar findings have been observed and there is a possibility that the peripheral neuropathy in SDT fatty rats would show similar histological findings to those in humans.

Glycemic control by phlorizin improved the functional abnormality of peripheral neuropathy, the reduction of nerve density in the epidermis, and morphological abnormality and vacuolation of the mitochondria of the sciatic nerve (Chapter 2: Figures 3 to 6, Table 1). Good glycemic control, which was achieved by insulin treatment in STZ-induced diabetic mice and voglibose treatment in GK rats, has been reported to improve the neurological dysfunction and the pathological abnormalities (Yorek et al., 2014; Wada et al., 1999). In contrast, treatment with pioglitazone, a peroxisome proliferator-activated receptor γ (PPARγ) agonist, in ZDF rats has provided good glycemic control, but did not improve neurological function (Hempe et al., 2012).

This suggested that the sustained hyperglycemia may be involved in the development of peripheral neuropathy in SDT fatty rats.

Mechanism of Central Neuropathy

Dementia is a worldwide problem, including Japan, and it is estimated that the rate of occurrence will increase further. According to the World Alzheimer Report 2018, the world's dementia population is estimated to be 50 million at the time of 2018, but it will increase to 82 million by 2030 and to 152 million by 2050 (Patterson, 2018).

It is known that AD, the most common form of dementia, can be prevented to some extent by improvement of lifestyle such as exercise, sleep, or mental care, but robust treatment and effective preventive methods against AD have not been discovered yet. As mentioned in Chapter 1, DM is one of the risk factors for dementia, and the risk of developing AD is higher in DM patients. Considering various reports on the relevance to DM and dementia, SDT fatty rats established as an obese type 2 DM model may also have CNS abnormalities, but there has been no research on central neuropathy of SDT fatty rats. Therefore, in the present study, histopathological examination of the brain was conducted in aged rats, and the influence on the CNS was investigated.

In AD patients, morphological abnormalities such as cerebral atrophy have been reported based on MRI and postmortem brain studies (Frolich et al., 1998; Moran et al., 2015), while cortical volume and cortical thickness have also been reported as being decreased in type 2 DM patients without AD (den Heijer et al., 2003; Brundel et al., 2010). In the brain of SDT fatty rats, the thinned cerebral cortex and a decrease in the number of pyramidal cells in the hippocampal CA1 and CA3 regions of SDT fatty rats has been observed at 58 weeks of age (Chapter 3: Figure 8 to 10), but no effect was

observed at 32 weeks of age. This suggests that the sustained hyperglycemia might affect cortical thickness and the reduction of pyramidal cells. The hippocampus plays an important role in the mechanism of spatial, semantic, and episodic memory (Hoscheidt et al., 2010). Neuronal density of hippocampal CA1 and CA3 in AD patients is significantly reduced (Padurariu et al., 2012). The hippocampus is considered to be very fragile, and many CNS disorders such as dementia, schizophrenia, and Huntington's disease were found to be related to the loss of hippocampal neurons (Korbo et al., 2004; Gattaz et al., 2011; Walker et al., 2011). This reduction of nerve cells is a very interesting change and it is a strong suggestion of the possibility of being related to CNS disorders in view of the above reports.

In addition to morphological changes in the brain of SDT fatty rats, expression of inflammation-related genes in the brain has also been confirmed (Chapter 3: Figure 12). SDT fatty rats are hyperinsulinemic at young age (Chapter 2: Figure 2), since plasma insulin concentrations after 32 weeks of age are low (Chapter 3: Figure 7), and it is thought that insulin secretion failure occurs at higher age. It has been reported that insulin resistance, AGEs, oxidative stress, and inflammatory response are involved in cognitive dysfunction of DM patients (Muriach et al., 2014). Therefore, in the brain of SDT fatty rats, the occurrence of insulin resistance and inflammation accompanied by persistent hyperglycemia suggest a relationship with the morphological abnormality of the brain.

It has been shown that there is Aβ deposition in the brain in AD models associated with abnormal glucose metabolism (Jolivalt et al., 2010; Yang et al., 2017). However, amyloid deposition was not confirmed in the present study (Chapter 3: Figure 11). As mentioned in Chapter 1, dementia is caused by various diseases. There is

a possibility that SDT fatty rats may be distinct from AD with amyloid deposition. Until now, amyloid hypotheses were prevalent in AD, a typical disease causing dementia. However, many treatment strategies based on amyloid reduction have failed in clinical trials (Teich and Arancio, 2012). This failure has raised questions about the amyloid hypothesis itself. SDT fatty rats have the potential to contribute to the discovery of a novel mechanism of dementia that does not conform to the hypothesis of amyloid deposits.

Behavioral tests are performed to evaluate the learning and memory in the rodent models. For example, Morris water maze test, eight-arm radial maze test, Barnes maze test, new object recognition test, and Y maze are used: the latter three being less affected by stress (Morris, 1981; Olton and Samuelson, 1976; Barnes, 1979; Dodart et al., 1997; Hidaka et al., 2011). Attempts were made in the present study to evaluate cognitive function using Y maze in SDT fatty rats. However, when set to the evaluation device at the time of measurement, no exploratory behavior was observed, and many individuals were observed to gather at the same place, and therefore evaluation could not be made (data not shown). Behavioral evaluation of cognitive function in ZDF rats using Morris water maze has been reported (Belanger et al., 2004; Gu et al., 2017). Therefore, to evaluate the cognitive function of SDT fatty rats behaviorally, it may be worthwhile to use water maze for the evaluation.

Conclusion

SDT fatty rats developed the DPN from a relatively early stage, and it became clear that the disorder occurred in both somatic and autonomic nerves. Among the characteristics, sensory nerve dysfunction and autonomic dysfunction of the pupillary

reaction were clearly observed. Furthermore, mitochondrial abnormalities and vacuolation of the sciatic nerve were also morphologically observed, and thus morphological abnormalities were also revealed. Blood glucose control, the first choice of clinical treatment, was shown to be effective for DPN in this model rat, and the results support the involvement of hyperglycemia in DPN. Studies on the brain of aged SDT fatty rats also revealed that sustained hyperglycemia causes the histological abnormalities of the brain accompanied by the increased expression of inflammation-related genes. These results may contribute to the discovery of new therapies for DPN as well as CNS disorders. In the future, it will be important to analyze the sequential pathological changes and identify new therapeutic targets in the diabetic peripheral and central neuropathy.

Acknowledgements

I wish to express sincere appreciation to Shin-ichi Kume, Professor in Graduate School of Agriculture, Kyoto University, for his valuable advice and the kindest support and encouragements throughout this study. I am grateful to Miki Sugimoto and Shuntaro Ikeda, Assistant Professors in Graduate School of Agriculture, Kyoto University for their kind advice.

I would like to thank Dr. Shigenori Ohkawa and Dr. Mutsuyoshi Matsushita, from Japan Tobacco Inc. Central Pharmaceutical Research Institute for providing the opportunity to conduct this study. I would also like to express my gratitude to Dr. Takeshi Ohta, who provided constructive comments and suggestions, and would also like to thank Dr. Tomohiko Sasase, Mr. Hironobu Tadaki for their advice and involvement with parts of the experiments.

Finally, I want to thank my family to completion of this study.

References

Anderson, R.J., Freedland, K.E., Clouse, R.E., Lustman, P.J., 2001. The prevalence of comorbid depression in adults with diabetes: a meta-analysis. *Diabetes Care* **24**, 1069–1078.

Arimura, A., Deguchi, T., Sugimoto, K., Uto, T., Nakamura, T., Arimura, Y., Arimura, K., Yagihashi, S., Nishio, Y., Takashima, H., 2013. Intraepidermal nerve fiber density and nerve conduction study parameters correlate with clinical staging of diabetic polyneuropathy. *Diabetes Res Clin Pract* **99**, 24–29.

Asnaghi, V., Gerhardinger, C., Hoehn, T., Adeboje, A., Lorenzi, M., 2003. A role for the polyol pathway in the early neuroretinal apoptosis and glial changes induced by diabetes in the rat. *Diabetes* **52**, 506–511.

Barnes, C.A., 1979. Memory deficits associated with senescence: a neurophysiological and behavioral study in the rat. *J Comp Physiol Psychol* **93**, 74–104.

Belanger, A., Lavoie, N., Trudeau, F., Massicotte, G., Gagnon, S., 2004. Preserved LTP and water maze learning in hyperglycaemic-hyperinsulinemic ZDF rats. *Physiol Behav* **83**, 483–494.

Biessels, G.J., Staekenborg, S., Brunner, E., Brayne, C., Scheltens, P., 2006. Risk of dementia in diabetes mellitus: a systematic review. *Lancet Neurol* **5**, 64–74.

Bomfim, T.R., Forny-Germano, L., Sathler, L.B., Brito-Moreira, J., Houzel, J.C., Decker, H., Silverman, M.A., Kazi, H., Melo, H.M., McClean, P.L., Holscher, C., Arnold, S.E., Talbot, K., Klein, W.L., Munoz, D.P., Ferreira, S.T., De Felice, F.G.,

2012. An anti-diabetes agent protects the mouse brain from defective insulin signaling caused by Alzheimer's disease- associated Abeta oligomers. *J Clin Invest* **122**, 1339–1353.

Bowen, D.M., Smith, C.B., White, P., Davison, A.N., 1976. Neurotransmitter-related enzymes and indices of hypoxia in senile dementia and other abiotrophies. *Brain* **99**, 459–496.

Brands, A.M., Biessels, G.J., de Haan, E.H., Kappelle, L.J., Kessels, R.P., 2005. The effects of type 1 diabetes on cognitive performance: a meta-analysis. *Diabetes Care* **28**, 726–735.

Brundel, M., van den Heuvel, M., de Bresser, J., Kappelle, L.J., Biessels, G.J., Utrecht Diabetic Encephalopathy Study, G., 2010. Cerebral cortical thickness in patients with type 2 diabetes. *J Neurol Sci* **299**, 126–130.

Callaghan, B.C., Cheng, H.T., Stables, C.L., Smith, A.L., Feldman, E.L., 2012. Diabetic neuropathy: clinical manifestations and current treatments. *Lancet Neurol* **11**, 521–534.

Chen, L., Li, B., Chen, B., Shao, Y., Luo, Q., Shi, X., Chen, Y., 2016. Thymoquinone Alleviates the Experimental Diabetic Peripheral Neuropathy by Modulation of Inflammation. *Sci Rep* **6**, 31656.

Daugaard, M., Rohde, M., Jaattela, M., 2007. The heat shock protein 70 family: Highly homologous proteins with overlapping and distinct functions. *FEBS Lett* **581**, 3702–3710.

Davies, P., Maloney, A.J., 1976. Selective loss of central cholinergic neurons in

Alzheimer's disease. *Lancet* **2**, 1403.

de la Monte, S.M., Wands, J.R., 2008. Alzheimer's disease is type 3 diabetes-evidence reviewed. *J Diabetes Sci Technol* **2**, 1101–1113.

DeKosky, S.T., Scheff, S.W., 1990. Synapse loss in frontal cortex biopsies in Alzheimer's disease: correlation with cognitive severity. *Ann Neurol* **27**, 457–464.

den Heijer, T., Vermeer, S.E., van Dijk, E.J., Prins, N.D., Koudstaal, P.J., Hofman, A., Breteler, M.M., 2003. Type 2 diabetes and atrophy of medial temporal lobe structures on brain MRI. *Diabetologia* **46**, 1604–1610.

Dinel, A.L., Andre, C., Aubert, A., Ferreira, G., Laye, S., Castanon, N., 2011. Cognitive and emotional alterations are related to hippocampal inflammation in a mouse model of metabolic syndrome. *PLoS One* **6**, e24325.

Dodart, J.C., Mathis, C., Ungerer, A., 1997. Scopolamine-induced deficits in a two-trial object recognition task in mice. *Neuroreport* **8**, 1173–1178.

Drel, V.R., Mashtalir, N., Ilnytska, O., Shin, J., Li, F., Lyzogubov, V. V., Obrosova, I.G., 2006. The leptin-deficient (*ob/ob*) mouse: A new animal model of peripheral neuropathy of type 2 diabetes and obesity. *Diabetes* **55**, 3335–3343.

Duyckaerts, C., Delatour, B., Potier, M.C., 2009. Classification and basic pathology of Alzheimer disease. *Acta Neuropathol* **118**, 5–36.

Filho, O.A.R., Fazan, V.P.S., 2006. Streptozotocin induced diabetes as a model of phrenic nerve neuropathy in rats. *J Neurosci Methods* **151**, 131–138.

Freeman, O.J., Unwin, R.D., Dowsey, A.W., Begley, P., Ali, S., Hollywood, K.A.,

Rustogi, N., Petersen, R.S., Dunn, W.B., Cooper, G.J., Gardiner, N.J., 2016. Metabolic Dysfunction Is Restricted to the Sciatic Nerve in Experimental Diabetic Neuropathy. *Diabetes* **65**, 228–238.

Frolich, L., Blum-Degen, D., Bernstein, H.G., Engelsberger, S., Humrich, J., Laufer, S., Muschner, D., Thalheimer, A., Turk, A., Hoyer, S., Zochling, R., Boissl, K.W., Jellinger, K., Riederer, P., 1998. Brain insulin and insulin receptors in aging and sporadic Alzheimer's disease. *J Neural Transm* **105**, 423–438.

Gabbay, K.H., Merola, L.O., Field, R.A., 1966. Sorbitol pathway: presence in nerve and cord with substrate accumulation in diabetes. *Science* **151**, 209–210.

Galuppo, M., Giacoppo, S., Bramanti, P., Mazzon, E., 2014. Use of natural compounds in the management of diabetic peripheral neuropathy. *Molecules* **19**, 2877–2895.

Gattaz, W.F., Valente, K.D., Raposo, N.R., Vincentiis, S., Talib, L.L., 2011. Increased PLA2 activity in the hippocampus of patients with temporal lobe epilepsy and psychosis. *J Psychiatr Res* **45**, 1617–1620.

Gaudieri, P.A., Chen, R., Greer, T.F., Holmes, C.S., 2008. Cognitive function in children with type 1 diabetes: a meta-analysis. *Diabetes Care* **31**, 1892–1897.

Gemmell, E., Bosomworth, H., Allan, L., Hall, R., Khundakar, A., Oakley, A.E., Deramecourt, V., Polvikoski, T.M., O'Brien, J.T., Kalaria, R.N., 2012. Hippocampal neuronal atrophy and cognitive function in delayed poststroke and aging-related dementias. *Stroke* **43**, 808–814.

Gibran, N.S., Jang, Y.C., Isik, F.F., Greenhalgh, D.G., Muffley, L.A., Underwood, R.A., Usui, M.L., Larsen, J., Smith, D.G., Bunnett, N., Ansel, J.C., Olerud, J.E., 2002.

Diminished neuropeptide levels contribute to the impaired cutaneous healing response associated with diabetes mellitus. *J Surg Res* **108**, 122–128.

Giugliano, D., Ceriello, A., Paolisso, G., 1996. Oxidative stress and diabetic vascular complications. *Diabetes Care* **19**, 257–267.

Gu, C., Zhou, W., Wang, W., Xiang, H., Xu, H., Liang, L., Sui, H., Zhan, L., Lu, X., 2017. ZiBuPiYin recipe improves cognitive decline by regulating gut microbiota in Zucker diabetic fatty rats. *Oncotarget* **8**, 27693–27703.

Ha, T.Y., Chang, K.A., Kim, J., Kim, H.S., Kim, S., Chong, Y.H., Suh, Y.H., 2010. S100a9 knockdown decreases the memory impairment and the neuropathology in Tg2576 mice, AD animal model. *PLoS One* **5**, e8840.

Han, C., 2017. Modified parasympathetic nervous system in Goto-Kakizaki diabetic rats. *Hirosaki Med J* **68**, 33–43.

Hempe, J., Elvert, R., Schmidts, H.L., Kramer, W., Herling, A.W., 2012. Appropriateness of the Zucker Diabetic Fatty rat as a model for diabetic microvascular late complications. *Lab Anim* **46**, 32–39.

Hermani, A., De Servi, B., Medunjanin, S., Tessier, P.A., Mayer, D., 2006. S100A8 and S100A9 activate MAP kinase and NF-kappaB signaling pathways and trigger translocation of RAGE in human prostate cancer cells. *Exp Cell Res* **312**, 184–197.

Hidaka, N., Suemaru, K., Takechi, K., Li, B., Araki, H., 2011. Inhibitory effects of valproate on impairment of Y-maze alternation behavior induced by repeated electroconvulsive seizures and c-Fos protein levels in rat brains. *Acta Med Okayama* **65**, 269–277.

Hinder, L.M., Vincent, A.M., Hayes, J.M., McLean, L.L., Feldman, E.L., 2013. Apolipoprotein E knockout as the basis for mouse models of dyslipidemia-induced neuropathy. *Exp Neurol* **239**, 102–110.

Ho, E.C., Lam, K.S., Chen, Y.S., Yip, J.C., Arvindakshan, M., Yamagishi, S., Yagihashi, S., Oates, P.J., Ellery, C.A., Chung, S.S., Chung, S.K., 2006. Aldose reductase-deficient mice are protected from delayed motor nerve conduction velocity, increased c-Jun NH2-terminal kinase activation, depletion of reduced glutathione, increased superoxide accumulation, and DNA damage. *Diabetes* **55**, 1946–1953.

Ho, L., Qin, W., Pompl, P.N., Xiang, Z., Wang, J., Zhao, Z., Peng, Y., Cambareri, G., Rocher, A., Mobbs, C. V, Hof, P.R., Pasinetti, G.M., 2004. Diet-induced insulin resistance promotes amyloidosis in a transgenic mouse model of Alzheimer's disease. *FASEB J* **18**, 902–904.

Ho, N., Sommers, M.S., Lucki, I., 2013. Effects of diabetes on hippocampal neurogenesis: links to cognition and depression. *Neurosci Biobehav Rev* **37**, 1346–1362.

Horikoshi, Y., Mori, T., Maeda, M., Kinoshita, N., Sato, K., Yamaguchi, H., 2004. Aβ N-terminal-end specific antibody reduced β-amyloid in Alzheimer-model mice. *Biochem Biophys Res Commun* **325**, 384–387.

Hoscheidt, S.M., Nadel, L., Payne, J., Ryan, L., 2010. Hippocampal activation during retrieval of spatial context from episodic and semantic memory. *Behav Brain Res* **212**, 121–132.

Hosseini, A., Abdollahi, M., 2013. Diabetic neuropathy and oxidative stress: therapeutic perspectives. *Oxid Med Cell Longev* **2013**, 168039.

Hotta, N., Kawamori, R., Atsumi, Y., Baba, M., Kishikawa, H., Nakamura, J., Oikawa, S., Yamada, N., Yasuda, H., Shigeta, Y., 2008. Stratified analyses for selecting appropriate target patients with diabetic peripheral neuropathy for long-term treatment with an aldose reductase inhibitor, epalrestat. *Diabet Med* **25**, 818–825.

Hsiao, K., Chapman, P., Nilsen, S., Eckman, C., Harigaya, Y., Younkin, S., Yang, F., Cole, G., 1996. Correlative memory deficits, Abeta elevation, and amyloid plaques in transgenic mice. *Science* **274**, 99–102.

Hu, G., Jousilahti, P., Bidel, S., Antikainen, R., Tuomilehto, J., 2007. Type 2 diabetes and the risk of Parkinson's disease. *Diabetes Care* **30**, 842–847.

Huber, M.J., Smith, S.A., Smith, S.E., 1985. Mydriatic drugs for diabetic patients. *Br J Ophthalmol* **69**, 425–427.

Iizuka, S., Suzuki, W., Tabuchi, M., Nagata, M., Imamura, S., Kobayashi, Y., Kanitani, M., Yanagisawa, T., Kase, Y., Takeda, S., Aburada, M., Takahashi, K.W., 2005. Diabetic complications in a new animal model (TSOD mouse) of spontaneous NIDDM with obesity. *Exp Anim* **54**, 71–83.

Ishii, Y., Maki, M., Yamamoto, H., Sasase, T., Kakutani, M., Ohta, T., 2010a. Evaluation of blood pressure in Spontaneously Diabetic Torii-*Lepr(fa)* rats. *Exp Anim* **59**, 525–529.

Ishii, Y., Ohta, T., Sasase, T., Morinaga, H., Ueda, N., Hata, T., Kakutani, M., Miyajima, K., Katsuda, Y., Masuyama, T., Shinohara, M., Matsushita, M., 2010b.

Pathophysiological analysis of female Spontaneously Diabetic Torii fatty rats. *Exp Anim* **59**, 73–84.

Ishii, Y., Motohashi, Y., Muramatsu, M., Katsuda, Y., Miyajima, K., Sasase, T., Yamada, T., Matsui, T., Kume, S., Ohta, T., 2015. Female spontaneously diabetic Torii fatty rats develop nonalcoholic steatohepatitis-like hepatic lesions. *World J Gastroenterol* **21**, 9067–9078.

Islam, M.S., 2013. Animal models of diabetic neuropathy: Progress since 1960s. *J. Diabetes Res* **2013**.

Jakobsen, J., Christiansen, J.S., Kristoffersen, I., Christensen, C.K., Hermansen, K., Schmitz, A., Mogensen, C.E., 1988. Autonomic and somatosensory nerve function after 2 years of continuous subcutaneous insulin infusion in type I diabetes. *Diabetes* **37**, 452–455.

Jiang, L.Y., Tang, S.S., Wang, X.Y., Liu, L.P., Long, Y., Hu, M., Liao, M.X., Ding, Q.L., Hu, W., Li, J.C., Hong, H., 2012. PPARgamma agonist pioglitazone reverses memory impairment and biochemical changes in a mouse model of type 2 diabetes mellitus. *CNS Neurosci Ther* **18**, 659–666.

Jolivalt, C.G., Hurford, R., Lee, C.A., Dumaop, W., Rockenstein, E., Masliah, E., 2010. Type 1 diabetes exaggerates features of Alzheimer's disease in APP transgenic mice. *Exp Neurol* **223**, 422–431.

Karavanaki, K., Davies, A.G., Hunt, L.P., Morgan, M.H., Baum, J.D., 1994. Pupil size in diabetes. *Arch Dis Child* **71**, 511–515.

Katsuda, Y., Ohta, T., Miyajima, K., Kemmochi, Y., Sasase, T., Tong, B., Shinohara,

M., Yamada, T., 2014. Diabetic complications in obese type 2 diabetic rat models. *Exp Anim* **63**, 121–132.

Katsuda, Y., Sasase, T., Tadaki, H., Mera, Y., Motohashi, Y., Kemmochi, Y., Toyoda, K., Kakimoto, K., Kume, S., Ohta, T., 2015. Contribution of hyperglycemia on diabetic complications in obese type 2 diabetic SDT fatty rats: effects of SGLT inhibitor phlorizin. *Exp Anim* **64**, 161–169.

Kennedy, W.R., Wendelschafer-Crabb, G., Johnson, T., 1996. Quantitation of epidermal nerves in diabetic neuropathy. *Neurology* **47**, 1042–1048.

Korbo, L., Amrein, I., Lipp, H.P., Wolfer, D., Regeur, L., Oster, S., Pakkenberg, B., 2004. No evidence for loss of hippocampal neurons in non-Alzheimer dementia patients. *Acta Neurol Scand* **109**, 132–139.

Kumar, A., Kaundal, R.K., Iyer, S., Sharma, S.S., 2007. Effects of resveratrol on nerve functions, oxidative stress and DNA fragmentation in experimental diabetic neuropathy. *Life Sci* **80**, 1236–1244.

Leibson, C.L., Rocca, W.A., Hanson, V.A., Cha, R., Kokmen, E., O'Brien, P.C., Palumbo, P.J., 1997. Risk of dementia among persons with diabetes mellitus: a population-based cohort study. *Am J Epidemiol* **145**, 301–308.

Li, X., Song, D., Leng, S.X., 2015. Link between type 2 diabetes and Alzheimer's disease: from epidemiology to mechanism and treatment. *Clin Interv Aging* **10**, 549–560.

Li, Z.-G., Zhang, W., Grunberger, G., Sima, A.A., 2002. Hippocampal neuronal apoptosis in type 1 diabetes. *Brain Res* **946**, 221–231.

Li, Z.G., Zhang, W., Sima, A.A., 2007. Alzheimer-like changes in rat models of spontaneous diabetes. *Diabetes* **56**, 1817–1824.

Livak, K.J., Schmittgen, T.D., 2001. Analysis of relative gene expression data using real-time quantitative PCR and the 2(-Delta Delta C(T)) Method. *Methods* **25**, 402–408.

Maekawa, T., Tadaki, H., Sasase, T., Motohashi, Y., Miyajima, K., Ohta, T., Kume, S., 2017. Pathophysiological profiles of SDT fatty rats, a potential new diabetic peripheral neuropathy model. *J Pharmacol Toxicol Methods* **88**, 160–166.

Mansilla, M.J., Comabella, M., Rio, J., Castillo, J., Castillo, M., Martin, R., Montalban, X., Espejo, C., 2014. Up-regulation of inducible heat shock protein-70 expression in multiple sclerosis patients. *Autoimmunity* **47**, 127–133.

Masuyama, T., Katsuda, Y., Shinohara, M., 2005. A novel model of obesity-related diabetes: introgression of the Lepr(fa) allele of the Zucker fatty rat into nonobese Spontaneously Diabetic Torii (SDT) rats. *Exp Anim* **54**, 13–20.

Matsuda, M., Hoshino, T., Yamashita, Y., Tanaka, K., Maji, D., Sato, K., Adachi, H., Sobue, G., Ihn, H., Funasaka, Y., Mizushima, T., 2010. Prevention of UVB radiation-induced epidermal damage by expression of heat shock protein 70. *J Biol Chem* **285**, 5848–5858.

Matsui, K., Ohta, T., Oda, T., Sasase, T., Ueda, N., Miyajima, K., Masuyama, T., Shinohara, M., Matsushita, M., 2008. Diabetes-associated complications in Spontaneously Diabetic Torii fatty rats. *Exp Anim* **57**, 111–21.

Miyamoto, M., Shintani, M., Nagaoka, A., Nagawa, Y., 1985. Lesioning of the rat basal

forebrain leads to memory impairments in passive and active avoidance tasks. *Brain Res* **328**, 97–104.

Moran, C., Beare, R., Phan, T.G., Bruce, D.G., Callisaya, M.L., Srikanth, V., Alzheimer's Disease Neuroimaging, I., 2015. Type 2 diabetes mellitus and biomarkers of neurodegeneration. *Neurology* **85**, 1123–1130.

Moran, C., Phan, T.G., Chen, J., Blizzard, L., Beare, R., Venn, A., Munch, G., Wood, A.G., Forbes, J., Greenaway, T.M., Pearson, S., Srikanth, V., 2013. Brain atrophy in type 2 diabetes: regional distribution and influence on cognition. *Diabetes Care* **36**, 4036–4042.

Morris, R.G.M., 1981. Spatial localization does not require the presence of local cues. *Learn Motiv* **12**, 239–260.

Motohashi, Y., Kemmochi, Y., Maekawa, T., Tadaki, H., Sasase, T., Tanaka, Y., Kakehashi, A., Yamada, T., Ohta, T., 2018. Diabetic macular edema-like ocular lesions in male spontaneously diabetic torii fatty rats. *Physiol Res* **67**, 423–432.

Murai, Y., Ohta, T., Tadaki, H., Miyajima, K., Shinohara, M., Fatchiyah, F., Yamada, T., 2017. Assessment of Pharmacological Responses to an Anti-diabetic Drug in a New Obese Type 2 Diabetic Rat Model. *Med Arch* **71**, 380–384.

Murakami, T., Iwanaga, T., Ogawa, Y., Fujita, Y., Sato, E., Yoshitomi, H., Sunada, Y., Nakamura, A., 2013. Development of sensory neuropathy in streptozotocin-induced diabetic mice. *Brain Behav* **3**, 35–41.

Murakawa, Y., Zhang, W., Pierson, C.R., Brismar, T., Östenson, C.G., Sima, A.A.F., 2002. Impaired glucose tolerance and insulinopenia in the GK-rat causes peripheral

neuropathy. *Diabetes Metab Res Rev* **18**, 473–483.

Muriach, M., Flores-Bellver, M., Romero, F.J., Barcia, J.M., 2014. Diabetes and the brain: oxidative stress, inflammation, and autophagy. *Oxid Med Cell Longev* **2014**, 102158.

Nakamura, J., Hamada, Y., Sakakibara, F., Hara, T., Wakao, T., Mori, K., Nakashima, E., Naruse, K., Kamijo, M., Koh, N., Hotta, N., 2001. Physiological and morphometric analyses of neuropathy in sucrose-fed OLETF rats. *Diabetes Res Clin Pract* **51**, 9–20.

Nomoto, S., Miyake, M., Ohta, M., Funakoshi, A., Miyasaka, K., 1999. Impaired learning and memory in OLETF rats without cholecystokinin (CCK)-A receptor. *Physiol Behav* **66**, 869–872.

Ogawa, K., Sasaki, H., Yamasaki, H., Okamoto, K., Matsuno, S., Shono, T., Doi, T., Arimoto, K., Furuta, H., Nishi, M., Nakao, T., Nanjo, K., 2006. Peripheral nerve functions may deteriorate parallel to the progression of microangiopathy in diabetic patients. *Nutr Metab Cardiovasc Dis* **16**, 313–321.

Ohara, T., Doi, Y., Ninomiya, T., Hirakawa, Y., Hata, J., Iwaki, T., Kanba, S., Kiyohara, Y., 2011. Glucose tolerance status and risk of dementia in the community: the Hisayama study. *Neurology* **77**, 1126–1134.

Ohkubo, Y., Kishikawa, H., Araki, E., Miyata, T., Isami, S., Motoyoshi, S., Kojima, Y., Furuyoshi, N., Shichiri, M., 1995. Intensive insulin therapy prevents the progression of diabetic microvascular complications in Japanese patients with non-insulin-dependent diabetes mellitus: a randomized prospective 6-year study.

Diabetes Res Clin Pract **28**, 103–117.

Ohta, T., Katsuda, Y., Miyajima, K., Sasase, T., Kimura, S., Tong, B., Yamada, T., 2014. Gender differences in metabolic disorders and related diseases in Spontaneously Diabetic Torii-Lepr(fa) rats. *J Diabetes Res* **2014**, 841957.

Olton, D.S., Samuelson, R.J., 1976. Remembrance of places passed: Spatial memory in rats. *J Exp Psychol Anim Behav Process* **2**, 97–116.

Ott, A., Stolk, R.P., van Harskamp, F., Pols, H.A., Hofman, A., Breteler, M.M., 1999. Diabetes mellitus and the risk of dementia: The Rotterdam Study. *Neurology* **53**, 1937–1942.

Padurariu, M., Ciobica, A., Mavroudis, I., Fotiou, D., Baloyannis, S., 2012. Hippocampal neuronal loss in the CA1 and CA3 areas of Alzheimer's disease patients. *Psychiatr Danub* **24**, 152–158.

Pahl, H.L., 1999. Activators and target genes of Rel/NF-kappaB transcription factors. *Oncogene* **18**, 6853–6866.

Partanen, J., Niskanen, L., Lehtinen, J., Mervaala, E., Siitonen, O., Uusitupa, M., 1995. Natural history of peripheral neuropathy in patients with non-insulin-dependent diabetes mellitus. *N Engl J Med* **333**, 89–94.

Patterson, C., 2018. World Alzheimer Report 2018: The state of the art of dementia research:New frontiers. London: Alzheimer's Disease International. *World Alzheimer Rep. 2018.*

Peila, R., Rodriguez, B.L., Launer, L.J., Honolulu-Asia Aging, S., 2002. Type 2 diabetes, APOE gene, and the risk for dementia and related pathologies: The

Honolulu-Asia Aging Study. *Diabetes* **51**, 1256–1262.

Pirart, J., 1978. Diabetes Mellitus and Its Degenerative Complications: A Prospective Study of 4,400 Patients Observed Between 1947 and 1973. *Diabetes Care* **1**, 168-188.

Pittenger, G.L., Ray, M., Burcus, N.I., McNulty, P., Basta, B., Vinik, A.I., 2004. Intraepidermal nerve fibers are indicators of small-fiber neuropathy in both diabetic and nondiabetic patients. *Diabetes Care* **27**, 1974–9.

Pop-Busui, R., Boulton, A.J., Feldman, E.L., Bril, V., Freeman, R., Malik, R.A., Sosenko, J.M., Ziegler, D., 2017. Diabetic Neuropathy: A Position Statement by the American Diabetes Association. *Diabetes Care* **40**, 136–154.

Pop-Busui, R., Lu, J., Lopes, N., Jones, T.L., Investigators, B. 2D, 2009. Prevalence of diabetic peripheral neuropathy and relation to glycemic control therapies at baseline in the BARI 2D cohort. *J Peripher Nerv Syst* **14**, 1–13.

Ramos-Rodriguez, J.J., Molina-Gil, S., Ortiz-Barajas, O., Jimenez-Palomares, M., Perdomo, G., Cozar-Castellano, I., Lechuga-Sancho, A.M., Garcia-Alloza, M., 2014. Central proliferation and neurogenesis is impaired in type 2 diabetes and prediabetes animal models. *PLoS One* **9**, 1–8.

Rickmann A, Waizel M, Kazerounian S, Szurman P, B.K., 2016. Relation of Pupil Size and retinal diseases. *Int J Ophthalmol Eye Sci* **4**, 242–245.

Saini, A.K., Kumar, H.S.A., Sharma, S.S., 2007. Preventive and curative effect of edaravone on nerve functions and oxidative stress in experimental diabetic neuropathy. *Eur J Pharmacol* **568**, 164–172.

Sakimura, K., Maekawa, T., Sasagawa, K., Ishii, Y., Kume, S.I., Ohta, T., 2018. Depression-related behavioural and neuroendocrine changes in the Spontaneously Diabetic Torii (SDT) fatty rat, an animal model of Type 2 Diabetes Mellitus. *Clin Exp Pharmacol Physiol* **45**, 927-933.

Sameni, H., Panahi, M., 2011. The effect of co-administration of 4-methylcatechol and progesterone on sciatic nerve function and neurohistological alterations in streptozotocin- induced diabetic neuropathy in rats. *Cell J* **13**, 31–38.

Shepherd, C.E., Goyette, J., Utter, V., Rahimi, F., Yang, Z., Geczy, C.L., Halliday, G.M., 2006. Inflammatory S100A9 and S100A12 proteins in Alzheimer's disease. *Neurobiol Aging* **27**, 1554–1563.

Shun, C.T., Chang, Y.C., Wu, H.P., Hsieh, S.C., Lin, W.M., Lin, Y.H., Tai, T.Y., Hsieh, S.T., 2004. Skin denervation in type 2 diabetes: correlations with diabetic duration and functional impairments. *Brain* **127**, 1593–1605.

Sigsbee, B., Torkelson, R., Kadis, G., Wright, J.W., Reeves, A.G., 1974. Parasympathetic denervation of the iris in diabetes mellitus. *A Clin study* **37**, 1031–1035.

Skovronsky, D.M., Zhang, B., Kung, M.P., Kung, H.F., Trojanowski, J.Q., Lee, V.M., 2000. In vivo detection of amyloid plaques in a mouse model of Alzheimer's disease. *Proc Natl Acad Sci U S A* **97**, 7609–7614.

Strachan, M.W., Deary, I.J., Ewing, F.M., Frier, B.M., 1997. Is type II diabetes associated with an increased risk of cognitive dysfunction? A critical review of published studies. *Diabetes Care* **20**, 438–445.

Stranahan, A.M., 2015. Models and mechanisms for hippocampal dysfunction in obesity and diabetes. *Neuroscience* **309**, 125–139.

Sumner, C.J., Sheth, S., Griffin, J.W., Cornblath, D.R., Polydefkis, M., 2003. The spectrum of neuropathy in diabetes and impaired glucose tolerance. *Neurology* **60**, 108–111.

Takeda, T., Hosokawa, M., Takeshita, S., Irino, M., Higuchi, K., Matsushita, T., Tomita, Y., Yasuhira, K., Hamamoto, H., Shimizu, K., Ishii, M., Yamamuro, T., 1981. A new murine model of accelerated senescence. *Mech Ageing Dev* **17**, 183–194.

Tanaka, M., Asanuma, A., Ikuta, J., Yamada, H., Shimizu, S., Koga, T., Kakishita, T., 1995. [Age-related memory impairment and hippocampal damage in ddY male mice]. *Exp Anim* **43**, 697–702.

Teich, A.F., Arancio, O., 2012. Is the amyloid hypothesis of Alzheimer's disease therapeutically relevant? *Biochem J* **446**, 165–177.

Tesfaye, S., Chaturvedi, N., Eaton, S.E., Ward, J.D., Manes, C., Ionescu-Tirgoviste, C., Witte, D.R., Fuller, J.H., Group, E.P.C.S., 2005. Vascular risk factors and diabetic neuropathy. *N Engl J Med* **352**, 341–350.

The Diabetes Control and Complications Trial Research Group, 1988. Factors in development of diabetic neuropathy. Baseline analysis of neuropathy in feasibility phase of Diabetes Control and Complications Trial (DCCT). *Diabetes* **37**, 476–481.

The Diabetes Control and Complications Trial Research Group, 1993. The effect of intensive treatment of diabetes on the development and progression of long-term

complications in insulin-dependent diabetes mellitus. *N Engl J Med* **329**, 977–986.

The Diabetes Control and Complications Trial Research Group, 1995. The effect of intensive diabetes therapy on the development and progression of neuropathy. *Ann Intern Med* **122**, 561–568.

Vareniuk, I., Pavlov, I.A., Obrosova, I.G., 2008. Inducible nitric oxide synthase gene deficiency counteracts multiple manifestations of peripheral neuropathy in a streptozotocin-induced mouse model of diabetes. *Diabetologia* **51**, 2126–2133.

Vincent, A.M., Feldman, E.L., 2004. New insights into the mechanisms of diabetic neuropathy. *Rev Endocr Metab Disord* **5**, 227–236.

Wada, R., Koyama, M., Mizukami, H., Odaka, H., Ikeda, H., Yagihashi, S., 1999. Effects of long-term treatment with alpha-glucosidase inhibitor on the peripheral nerve function and structure in Goto-Kakizaki rats: a genetic model for type 2 diabetes. *Diabetes Metab Res Rev* **15**, 332–337.

Walker, T.L., Turnbull, G.W., Mackay, E.W., Hannan, A.J., Bartlett, P.F., 2011. The latent stem cell population is retained in the hippocampus of transgenic Huntington's disease mice but not wild-type mice. *PLoS One* **6**, e18153.

Wang, J.Q., Yin, J., Song, Y.F., Zhang, L., Ren, Y.X., Wang, D.G., Gao, L.P., Jing, Y.H., 2014. Brain aging and AD-like pathology in streptozotocin-induced diabetic rats. *J Diabetes Res* **2014**, 796840.

West, M.J., Coleman, P.D., Flood, D.G., Troncoso, J.C., 1994. Differences in the pattern of hippocampal neuronal loss in normal ageing and Alzheimer's disease. *Lancet* **344**, 769–772.

Wrighten, S.A., Piroli, G.G., Grillo, C.A., Reagan, L.P., 2009. A look inside the diabetic brain: Contributors to diabetes-induced brain aging. *Biochim Biophys Acta* **1792**, 444–453.

Yagihashi, S., Matsunaga, M., 1979. Ultrastructural pathology of peripheral nerves in patients with diabetic neuropathy. *Tohoku J Exp Med* **129**, 357–366.

Yagihashi, S., Mizukami, H., Sugimoto, K., 2011. Mechanism of diabetic neuropathy: Where are we now and where to go? *J Diabetes Investig* **2**, 18–32.

Yagihashi, S., Wada, R., Kamijo, M., Nagai, K., 1993. Peripheral neuropathy in the WBN/Kob rat with chronic pancreatitis and spontaneous diabetes. *Lab Invest* **68**, 296–307.

Yamaguchi, T., Sasase, T., Mera, Y., Tomimoto, D., Tadaki, H., Kemmochi, Y., Ohta, T., Sato, E., Matsushita, M., 2012. Diabetic peripheral neuropathy in Spontaneously Diabetic Torii-Lepr(fa) (SDT fatty) rats. *J Vet Med Sci* **74**, 1669–73.

Yang, S., Chen, Z., Cao, M., Li, R., Wang, Z., Zhang, M., 2017. Pioglitazone ameliorates Abeta42 deposition in rats with diet-induced insulin resistance associated with AKT/GSK3beta activation. *Mol Med Rep* **15**, 2588–2594.

Yates, K.F., Sweat, V., Yau, P.L., Turchiano, M.M., Convit, A., 2012. Impact of metabolic syndrome on cognition and brain: a selected review of the literature. *Arter. Thromb Vasc Biol* **32**, 2060–2067.

Yorek, M.S., Obrosov, A., Shevalye, H., Lupachyk, S., Harper, M.M., Kardon, R.H., Yorek, M.A., 2014. Effect of glycemic control on corneal nerves and peripheral

neuropathy in streptozotocin-induced diabetic C57Bl/6J mice. *J Peripher Nerv Syst* **19**, 205–217.

Yoshitake, T., Kiyohara, Y., Kato, I., Ohmura, T., Iwamoto, H., Nakayama, K., Ohmori, S., Nomiyama, K., Kawano, H., Ueda, K., et al., 1995. Incidence and risk factors of vascular dementia and Alzheimer's disease in a defined elderly Japanese population: the Hisayama Study. *Neurology* **45**, 1161–1168.

Yu, J.-X., Yin, X.-X., Shen, J.-P., Qiu, J., Yin, H., Jiang, S., 2006. Protective effects of bendazac lysine on diabetic peripheral neuropathy in streptozotocin-induced diabetic rats. *Clin Exp Pharmacol Physiol* **33**, 1231–8.

Zhou, J., Zhou, S., 2014. Inflammation: therapeutic targets for diabetic neuropathy. *Mol Neurobiol* **49**, 536–546.